Title: Auditory cortex shapes sound responses in the inferior colliculus.

Authors: Jennifer M. Blackwell[1,2], Alexandria Lesicko[1], Winnie Rao[1], Mariella De Biasi[3,4,5], Maria N. Geffen[1,5,6*]

Affiliation: [1]*Department of Otorhinolaryngology, University of Pennsylvania, Philadelphia, PA*
[2]*Department of Neurobiology and Behavior, Stony Brook University, Stony Brook, NY*
[3]*Department of Psychiatry, University of Pennsylvania, Philadelphia, PA*
[4]*Department of Systems Pharmacology and Experimental Therapeutics, University of Pennsylvania, Philadelphia, PA*
[5]*Department of Neuroscience, University of Pennsylvania, Philadelphia, PA*
[6]*Department of Neurology, University of Pennsylvania, Philadelphia, PA*

**** Corresponding Author:***
Maria N. Geffen, Ph.D.
Associate Professor
Department of Otorhinolaryngology
Department of Neuroscience
Department of Neurology
University of Pennsylvania
Stemmler Hall G14A
3450 Hamilton Walk
Philadelphia PA 19104
(215) 898-0782
mgeffen@pennmedicine.upenn.edu
http://www.med.upenn.edu/hearing

Abstract

The extensive feedback from the auditory cortex (AC) to the inferior colliculus (IC) supports critical aspects of auditory behavior but has not been extensively characterized. Previous studies demonstrated that activity in IC is altered by focal electrical stimulation and pharmacological inactivation of AC, but these methods lack the ability to selectively manipulate projection neurons. We measured the effects of selective optogenetic modulation of cortico-collicular feedback projections on IC sound responses in mice. Activation of feedback increased spontaneous activity and decreased stimulus selectivity in IC, whereas suppression had no effect. To further understand how microcircuits in AC may control collicular activity, we optogenetically modulated different cortical neuronal subtypes, specifically parvalbumin-positive (PV) and somatostatin-positive (SST) inhibitory interneurons. We found that modulating either type of interneuron did not affect IC sound-evoked activity. Combined, our results identify that activation of excitatory projections, but not inhibition-driven changes in cortical activity, affects collicular sound responses.

Introduction

Information processing is typically studied as a set of computations ascending along a hierarchy of sensory areas, often overlooking the role of descending feedback between these nuclei. In the auditory system, the auditory cortex (AC) sends extensive feedback to nuclei earlier in the auditory pathway, including the auditory thalamus (Alitto & Usrey, 2003; Rouiller & Durif, 2004; Winer, Diehl, & Larue, 2001) and the inferior colliculus (IC) (Bajo & Moore, 2005; Bajo, Nodal, Bizley, Moore, & King, 2007; Coomes, Schofield, & Schofield, 2005; Doucet, Molavi, & Ryugo, 2003; Saldaña, Feliciano, & Mugnaini, 1996; Winer, Larue, Diehl, & Hefti, 1998). Previous studies have demonstrated the importance of cortical feedback to IC in auditory behaviors (Bajo, Nodal, Moore, & King, 2010; Xiong et al., 2015), however, the mechanisms by which information processing is shaped via the *descending feedback* pathway remain poorly characterized. In this study, we selectively modulated activity in AC, targeting either excitatory projections or inhibitory interneurons, to quantify how AC shapes spontaneous activity and sound-evoked responses in IC.

Previous studies demonstrated that neuronal responses to sounds in IC are altered by focal electrical stimulation and inactivation of AC. Cortical stimulation shifted tuning properties of IC neurons toward those of the stimulated neurons in frequency (Jen et al., 1998; Jen & Zhou, 2003; Ma & Suga, 2001b; J. Yan, Zhang, Ehret, & Yan, 2005; W. Yan & Suga, 1998; X. Zhou & Jen, 2007), amplitude (Jen & Zhou, 2003; J. Yan et al., 2005; X. Zhou & Jen, 2007), azimuth (X. Zhou & Jen, 2007; Xiaoming Zhou & Jen, 2005), and duration (Ma & Suga, 2001a). Stimulation of AC had mixed effects on sound-evoked responses in IC, increasing and decreasing responses in different subpopulations of neurons (Jen et al., 1998; Xiaoming Zhou & Jen, 2005). Consistent with this effect, different patterns of direct cortico-collicular activation enhanced or suppressed white noise-induced responses in IC (Vila, Williamson, Hancock, & Polley, 2019). AC inactivation studies, on the other hand, found less consistent effects on IC responses. Whereas one study found inactivation of AC caused a shift in best frequency in IC neurons (Zhang, Suga, & Yan, 1997), several other studies showed that inactivation of AC had no effect on frequency selectivity in IC (Jen et al., 1998), but rather modulated sound-evoked and spontaneous activity (Gao & Suga, 1998; J Popelář, Nwabueze-Ogbo, & Syka, 2003; Jiří Popelář et al., 2016). Cortico-collicular feedback is critical to auditory learning, specifically learning to adapt to a unilateral earplug during sound localization (Bajo et al., 2010). Pairing electrical leg stimulation with a tone induced a shift in best frequency of IC neurons, while presentation of a tone alone was insufficient (Gao & Suga, 1998, 2000). Furthermore, cortico-collicular feedback was necessary to induce running in response to a loud noise (Xiong et al., 2015).

In AC, modulation of sound responses is not a monophasic process, but instead is shaped by interactions between excitatory and inhibitory cortical neurons. Modulating activity of different inhibitory interneuron subtypes in AC narrowed frequency tuning and attenuated tone-evoked responses of excitatory neurons, while suppression had the opposite effect (Aizenberg, Mwilambwe-Tshilobo, Briguglio, Natan, &

Geffen, 2015; Hamilton et al., 2013; Phillips & Hasenstaub, 2016; Seybold et al., 2015). Electrical stimulation of AC, cooling or pharmacological inactivation affected the amplitude of sound-evoked responses and shifted the best frequency of neurons in IC, but it remains unknown how specific these effects are to direct feedback, and whether the effects of intra-cortical inhibition propagate to the IC.

The goal of the present study is to examine the role of cortico-collicular projections in shaping sound responses in IC. IC receives glutamatergic (Feliciano & Potashner, 1995) inputs from neurons originating predominantly in layer 5 of AC (Bajo & Moore, 2005; Bajo et al., 2007; Coomes et al., 2005; Doucet et al., 2003; Saldaña et al., 1996; Winer et al., 1998). We used viral transfection methods to selectively drive excitatory or inhibitory opsin expression in AC-IC projections. We then recorded neuronal activity in IC and tested how activation or suppression of AC-IC projections affected spontaneous activity and sound-evoked responses in IC. To better understand whether and how intra-cortical network interactions propagated to IC, we manipulated the activity of the two most common inhibitory neuronal subtypes in AC, Parvalbumin-(PV) and Somatostatin-(SST) positive interneurons (Rudy, Fishell, Lee, & Hjerling-Leffler, 2011).

Results

Activating direct cortico-collicular feedback modulates activity in the inferior colliculus

Our first goal was to characterize the effects of activating the direct cortico-collicular projections on tone-evoked responses in IC. A combination of cortical anterograde and collicular retrograde viral transfections in order to achieve specific viral transfection of cortico-collicular neurons. We used a viral transfection strategy to deliver either an excitatory opsin, ChannelRhodopsin2 (ChR2) or an inhibitory opsin, ArchaerhodopsinT (ArchT), bilaterally, specifically to the neurons in the auditory cortex which project to the inferior colliculus (**Figure 1A**). To achieve such specificity, we injected a retrograde virus that encoded Cre recombinase (Retro2 AAV.Cre) in IC (**Figure 1B**). This retrograde viral construct ensured that neurons projecting to IC expressed Cre recombinase a few weeks later. At the same time, we injected a virus that encoded ChR2 or ArchT in reversed fashion under the FLEX cassette in AC (AAV.Flex.ChR2, AAV.Flex.ArchT) (**Figure 1C**). This strategy ensured that only neurons expressing Cre recombinase in the auditory cortex would express ChR2 or ArchT in AC. Therefore, opsin was expressed exclusively in AC-IC projecting neurons, which terminate across all regions of IC, including central nucleus (CNIC) and dorsal cortex of IC (DCIC), from which we recorded (**Figure 1D**). Shining light over AC of these mice would therefore directly activate or suppress only these cortico-collicular feedback projections to IC.

First, we measured and quantified neuronal spiking in IC in response to stimulation or suppression of cortico-collicular projections. To activate these neurons, we shone blue laser over AC, recorded neuronal activity in IC, and quantified the effects of manipulating feedback in the absence of sound (**Figure 2 C,D**). We

measured the spiking activity as we varied the duration of laser manipulation (1 ms, 5 ms, 25 ms, 250 ms). As expected, activation of cortico-collicular neurons resulted, on average, in an increase in firing rate of IC neurons. This effect persisted at the 5ms, 25ms, and 250ms laser duration (**Figure 2C**; *1 ms*: p = 5.3e-4, ON = 5.6 ± 0.6 Hz, OFF = 4.9 ± 0.5 Hz; *5 ms*: p = 0.0027, ON = 6.9 ± 0.7 Hz, OFF = 4.8 ± 0.5 Hz; *250 ms*: p = 0.005, ON = 5.6 ± 0.6 Hz, OFF = 4.8 ± 0.5 Hz). Whereas the direction of the effect was consistent with our prior expectations, the magnitude of the effect was unexpectedly small. This suggests that AC targets a small subpopulation of IC neurons and that the effect of activation does not spread too far within IC.

We tested the effect of suppressing AC-IC neurons on firing responses in IC and, surprisingly, we detected little difference in firing in IC neurons (**Figure 2D;** 2*5 ms*: p = 0.039, ON = 9.5 ± 0.7 Hz, OFF = 9.5 ± 0.7 Hz; *250 ms*: p = 0.02, ON = 9.5 ± 0.8 Hz, OFF = 9.5 ± 0.8 Hz). This result suggests that AC-IC inputs at rest do not contribute to IC responses, but rather modulate collicular activity only when activated.

Next, our goal was to characterize modulation of sound-evoked responses in IC by cortical feedback. We first tested the effects of feedback modulation on acoustic click responses. We chose clicks as the initial stimulus because they drive fast responses in both AC and IC. Laser stimulation began 250 ms prior to click train onset to allow for the response to the laser to come to a steady state, and continued activation throughout the clicks. Activating the feedback had a weak suppressive effect on the firing rate of IC neurons in response to clicks. Consistent with previous experiments, we observed an overall increase in spontaneous activity (**Figure 2E**, bottom; p = 0.0031, spont ON = 5 ± 0.87 Hz, spont OFF = 4.3 ± 0.92 Hz). Activating feedback caused a small decrease in click-evoked response (**Figure 2E**, left; p = 0.001, click ON = 10.4 ± 1.2 Hz, click OFF = 10.7 ± 1.1 Hz).

By contrast, suppressing cortico-collicular feedback using ArchT had no effect on IC click responses (**Figure 2F**). Because attenuating the input does not affect the activity in IC during clicks this result further suggests that the strength of the baseline signal from AC to IC, even in the presence of cortical activity, is not sufficient to modulate IC responses.

We also tested whether the effects of cortico-collicular modulation differed across the receptive field of collicular neurons. We presented a stimulus that consisted of tones of 50 frequencies ranging from 3 to 70 kHz. To modulate the feedback from AC, we tested three different laser onsets (-100 ms, -20 ms, +8 ms) relative to tone onset to isolate the effect of timing on affecting IC responses. These delays were chosen for the following reasons: -100ms delay would allow for the laser effect on cortical activity to come to a steady state, making it easier to quantify the effect throughout the tone pip; +8 ms is set up to mimic the time scale of cortical response to a tone, effectively amplifying the onset of the cortical response; -20 ms delay is an intermediate value.

We found that whereas activating feedback increased spontaneous activity of IC neurons (**Figure 3A**, left; -100 ms: p = 0.022, ON = 4.3 ± 0.47 Hz; OFF = 3.6 ± 0.38; -20 ms: p = 8.6e-6, ON = 5.6 ± 0.63, OFF =

3.7 ± 0.47), overall the feedback decreased tone-evoked response magnitude in IC, which we defined as the difference between spontaneous and tone-evoked response, at all laser onsets (**Figure 3A**, right; -100 ms: p = 3.2e-5, ON = 14.2 ± 0.98 Hz; OFF = 15.5 ± 1.04 Hz; -20 ms: p = 1.4e-6, ON = 11.8 ± 1.08 Hz, OFF = 13.9 ± 1 Hz; +8 ms: p = 0.0034, ON = 13.03 ± 1.03, OFF = 13.7 ± 1.03). This suggests that the broad activation of feedback upregulates the baseline activity of IC neurons, but decreases tone-evoked response (**Figure 6C, -*100ms***: p = 0.018, ON = 19.01 ± 1.2 Hz, OFF = 18.5 ± 1.2 Hz; *+8ms*: p = 0.007, ON = 17.3 ± 1.2 Hz; OFF = 16.9 ± 1.2 Hz). By contrast, suppressing the feedback had no effect on either spontaneous activity or tone-evoked response magnitude (**Figure 3B**), suggesting that at baseline, AC does not provide strong modulation of IC activity, as removing it does not affect sound-evoked effects in IC.

We then examined the effect of feedback on frequency tuning of IC units. Activation of feedback decreased frequency selectivity in the subsets of units that also showed a decrease in tone-evoked response magnitude or increase in spontaneous activity, but not in units that showed an increase in tone-evoked response magnitude or decrease in spontaneous activity (**Figure 4A**, mag decrease: -20 ms, p = 0.00031, sparse ON = 0.49 ± 0.027, sparse OFF = 0.55 ± 0.025; +8 ms, p = 0.00029, sparse ON = 0.46 ± 0.027, sparse OFF = 0.55 ± 0.024; spont increase: -100 ms, p = 0.011, sparse ON = 0.49 ± 0.032, sparse OFF = 0.56 ± 0.031; -20 ms, p = 0.00018, sparse ON = 0.46 ± 0.034, sparse OFF = 0.56 ± 0.029; +8 ms, p = 2.2e-6, sparse ON = 0.41 ± 0.032, sparse OFF = 0.55 ± 0.029).

Interestingly, these changes are observed almost exclusively in cells located in DCIC rather than CNIC (**Figure 5**). Specifically, activation of feedback increased spontaneous activity (**Figure 5A**, left; *-100 ms*: p = 0.0204, ON = 3.5 ± 0.5 Hz, OFF = 2.5 ± 0.3 Hz; *-20 ms*: p = 2.8e-7, ON = 5.2 ± 0.7 Hz, OFF = 2.3 ± 0.3 Hz) and decreased tone-evoked response magnitude (**Figure 5A**, right, *-100 ms*: p = 3.3e-6, ON = 14.8 ± 1.4 Hz, OFF = 16.5 ± 1.5 Hz; *-20 ms*: p = 6.3e-7, ON = 11.8 ± 1.6 Hz, OFF = 14.7 ± 1.4 Hz) in cells located in DCIC, but CNIC (**Figure 5B**). Similarly, activation of feedback decreased frequency selectivity (**Figure 5C**; mag decrease: *-20 ms*, p = 6.3e-4, sparse ON = 0.46 ± 0.03, sparse OFF = 0.53 ± 0.03; *+8 ms*, p = 4.7e-5, sparse ON = 0.41 ± 0.03, sparse OFF = 0.53 ± 0.03; spont increase: *-100 ms*, p = 0.0044, sparse ON = 0.43 ± 0.04, sparse OFF = 0.52 ± 0.04; *-20 ms*, p = 0.00013, sparse ON = 0.39 ± 0.04, sparse OFF = 0.53 ± 0.04; *+8 ms*, p = 5.2e-6, sparse ON = 0.33 ± 0.03, OFF = 0.53 ± 0.04) in cells located in DCIC, but not CNIC (**Figure 5D**). This is consistent with the enhanced density of AC projections in DCIC as compared to CNIC (**Figure 1D**). To verify these results were not due to a select few high firing units found in DCIC, we repeated the analysis comparing only units with spontaneous activity in the laser OFF condition less than 40 Hz. With these matched firing rates we still see the same statistically significant effects (DCIC – mag decrease -100 ms: p = 3.3e-6, ON = 14.8 Hz, OFF = 16.6 Hz; -20 ms: p = 6.3e-7, ON = 12.1 Hz, OFF = 12.6 Hz; spont increase -100 ms: p = 0.02 ON = 3.5 Hz, OFF = 2.5 Hz; -20 ms: p = 2.8e-7, ON = 5.1 Hz, OFF = 4.9 Hz; CNIC – mag decrease +8 ms: p = 0.0039, ON = 11.7 Hz, OFF = 12.6 Hz).

To elucidate changes in the shape of the frequency response curves beyond the general changes in selectivity we observe with changes in sparseness, we fit linear regressions to light off versus light on firing rates. This analysis can reveal whether changes in frequency selectivity are linear/subtractive, multiplicative/divisive, or some combination. For example, a slope of 1 and a positive y-intercept would represent a linear increase in frequency response (equal increase in response across all frequencies). Over the population of neurons with decreased tone-evoked response magnitude and/or increased spontaneous activity, the median slopes and y-intercepts of ranked linear fits to frequency responses are less than 1 and above zero, respectively (**Figure 6A**). These results, in combination with the decreased tone-evoked activity observed (**Figure 6B**, *-100ms*: $p = 0.018$, ON = 19.01 ± 1.2 Hz, OFF = 18.5 ± 1.2 Hz; *+8ms*: $p = 0.007$, ON = 17.3 ± 1.2 Hz; OFF = 16.9 ± 1.2 Hz), indicate the decrease in frequency selectivity was due to a decrease in response to tones at preferred frequencies, not non-preferred frequencies. This result suggests that the suppressive effect of the feedback is preferential for higher firing responses. Suppressing feedback resulted in very small (< 0.04 %) change in sparseness, therefore it did not affect frequency selectivity (**Figure 4B**).

Correlations in trial-to-trial responsiveness of neurons can affect the information encoded by a neuronal population (Abbott & Dayan, 1999; Averbeck, Latham, & Pouget, 2006; Nirenberg & Latham, 2003; Shadlen & Newsome, 1998; Zohary, Shadlen, & Newsome, 1994). To test whether activation of cortico-collicular feedback affected correlations in trial-to-trial variability of response strength between units recorded simultaneously we measured noise correlations. We found that activating cortico-collicular feedback had no effect on noise correlations during spontaneous activity or tone response (**Figure 3 - figure supplement 1**).

To better understand the effect of modulation of cortical activity on spectro-temporal receptive field properties of IC neurons, we presented a continuous signal comprised of dynamic random chords (DRCs) sampled from a uniform distribution of loudness values per frequency bin. The unbiased nature of this stimulus allowed us to estimate the spectro-temporal receptive field of neurons (STRF), which quantifies the dynamics of sound waveform in time and frequency that lead to a neuronal response. During the DRC stimulus, we turned on the laser every other second for 250 ms to either activate or suppress cortico-collicular projections. We found that a subset of cells reduced their mean DRC-evoked firing rates (N = 56), whereas another subset of cells increased their mean DRC-evoked firing rate when we activated cortico-collicular feedback (N = 47). We next separately computed the receptive fields for each neuron when laser was off and when laser was on and compared the STRFs. To quantify those changes, we identified the positive (activation) and negative (suppressive) regions in the STRFs and compared them for laser ON and laser OFF conditions. In the subset of neurons whose firing rate increased with laser STRFs changed: only 42% of positive lobes, and 63% of negative lobes persisted with the laser (**Figure 7B**, left). Of those lobes that persisted, for positive lobes, there was on average a decrease in temporal width ($p = 0.00098$, ON = 0.0303 ± 0.0018 s, OFF = 0.037 ± 0.0023 s), frequency selectivity ($p = 0.00042$, ON = 6.7 ± 1.1 Hz, OFF = 9.6 ± 1.8 Hz) and STRF size ($p = 0.00036$, ON

220 = 46.05 ± 6.9 pixels, OFF = 77.5 ± 12.04 pixels), whereas for negative lobes, we did not detect any changes
221 (**Figure 7C**, left). In neurons whose firing rate was decreased, there was a much smaller change in the lobes,
222 with 78% and 79% of positive and negative lobes persisting, respectively (**Figure 6B**, right). For both positive
223 lobes and negative lobes, the only difference was an increase in the temporal width when laser was activated
224 (**Figure 7C**, right; Positive lobes: p = 0.026, ON = 0.034 ±0.0025 s, OFF = 0.032 ± 0.0025 s; Negative lobes:
225 p = 0.02, ON = 0.037 ± 0.0028 s, OFF = 0.032 ± 0.0024 s). The decrease in STRF size in units with increased
226 DRC-evoked response and decrease in sparseness across the population is consistent with the interpretation
227 that the effect of the feedback leads to a decrease in responsiveness to tones that evoke the greatest responses
228 (in the center of the receptive field) and an increase to stimuli that evoke weaker activity. In other words,
229 neuronal firing increases overall, but selective responses to specific frequency bands decrease. Because the
230 majority of the units were recorded as multi-units, it is possible that this change in selectivity is due to the
231 change in firing rate of differentially tuned single units.
232
233 **Modulating inhibitory neuronal activity in AC does not affect collicular sound responses**
234 Auditory responses in AC are shaped by interactions between excitatory and inhibitory neurons (Wood,
235 Blackwell, & Geffen, 2017). To determine how modulating frequency selectivity in AC might affect tone-
236 evoked responses in IC in a frequency-selective fashion, we perturbed the excitatory-inhibitory interactions by
237 modulating two different classes of inhibitory interneuron known to contribute to sound responses in AC: PV
238 and SST inhibitory interneurons. We found that modulating PV interneuron activity in AC had little effect on
239 spontaneous and tone-evoked activity or frequency selectivity in IC (**Figure 8 B-E**) despite modulating
240 frequency selectivity, spontaneous activity, and tone-evoked response magnitude in AC. Specifically, in AC,
241 activating PVs decreased spontaneous activity and tone-evoked response magnitude (**Figure 8F**; spontaneous
242 activity: p = 2.2e-9, ON = 0.88 ± 0.16 Hz, OFF = 2.7 ± 0.34 Hz; tone-evoked response magnitude: p = 8.02e-
243 7, ON = 6.9 ± 1.06 Hz, OFF = 11.5 ± 1.3 Hz**)** and increased frequency selectivity (**Figure 8G**; p = 3.3e-12,
244 ON = 0.59 ± 0.022, OFF = 0.42 ± 0.02), while suppressing PVs increased spontaneous activity (**Figure 8I**; p
245 = 5.2e-5, ON = 4.08 ± 0.54 Hz, OFF = 3.06 ± 0.55 Hz) and decreased frequency selectivity (**Figure 8J**; p =
246 3.8e-5, ON = 0.34 ± 0.027, OFF = 0.41 ± 0.031). This suggests that the changes in cortical activity driven by
247 manipulation of PV activity does not propagate to the inferior colliculus.
248 Different interneuron classes may function in distinct networks, so we also tested the effects of
249 modulating SST interneurons. Modulating SST interneurons had no effect on tone-evoked activity (**Figure 9**
250 **B,D**, right) or frequency selectivity (**Figure 9 C,E**), but suppressing SST interneurons increased spontaneous
251 activity in IC (**Figure 9D**, left; p = 0.029, ON = 6.9 ± 0.66 Hz, OFF = 6.7 ± 0.63 Hz), a change that we also
252 observed with activation of the direct feedback projections (**Figure 2A**, left). Similar to PV interneurons,
253 activating SST interneurons decreased spontaneous activity and tone-evoked response magnitude in AC

(**Figure 9F**; spontaneous activity: p = 1.4e-12, ON = 0.97 ± 0.25 Hz, OFF = 2.9 ± 0.37 Hz; tone-evoked response magnitude: p = 1.3e-15, ON = 3.3 ± 0.59 Hz, OFF = 11.4 ± 1.2 Hz) and increased frequency selectivity (**Figure 9G**; p = 1.6e-13, ON = 0.69 ± 0.024, OFF = 0.47 ± 0.019). In AC, suppressing SSTs reduced spontaneous activity, but had no significant effect on tone-evoked response magnitude or frequency selectivity (**Figure 9 I,J**; p = 8.1e-4, ON = 3.6 ± 0.41 Hz, OFF = 2.2 ± 0.38 Hz). This lack of effect was not due to the relatively small effect of light penetrating to the deep layers. In fact, to confirm that modulating PV and SST activity in AC affected activity of units in L5/6 where the feedback projections we looked at changes in spontaneous activity at each tetrode which spanned the entire auditory cortex. We found that activity was modulated across the layers (**Figure 8-9 H,K**). Whereas modulating PVs did not have an effect on IC activity, SST suppression resulted in an increase in spontaneous, but not tone-evoked activity in IC, which suggests that inhibitory modulation of sound responses in AC does not propagate to IC.

Discussion

Auditory cortex sends extensive projections to IC (Bajo & Moore, 2005; Bajo et al., 2007; Coomes et al., 2005; Doucet et al., 2003; Saldaña et al., 1996; Winer et al., 1998). Our results demonstrate that activation of this cortico-collicular feedback modulates sound responses in IC by upregulating spontaneous IC activity, but decreasing frequency selectivity and reducing spectro-temporal receptive field size in IC. This effect was localized to DCIC, corresponding to the sites with largest density of AC projections. Interestingly, suppressing cortico-collicular feedback had little effect on IC activity, which suggests that at baseline and during passive tone presentation the feedback does not affect activity of IC neurons. We also found that SST, but not PV inhibitory interneurons modulated IC activity, suggesting that the effects of modulation of cortical activity by PVs does not back-propagate to IC, whereas SST-driven modulation affects spontaneous activity, but not tone-evoked responses. Overall our findings imply that direct cortico-collicular feedback can modulate responses to simple (pure tones) and more complex (DRCs) auditory stimuli by reducing, rather than increasing, sound selectivity. This modulation occurs independently of the activity of cortical inhibitory interneurons.

Whereas optogenetic manipulation allows for temporally precise control and cell-type specificity, the technique lacks the spatial specificity of electrical stimulation. Since both AC and cortico-collicular projections are tonotopically organized (Barnstedt, Keating, Weissenberger, King, & Dahmen, 2015; Lim & Anderson, 2007; Markovitz, Tang, & Lim, 2013; Straka, Hughes, Lee, & Lim, 2015), spatially specific stimulation can more accurately mimic frequency-specific responses by activating specific regions in the tonotopic map. Previous studies found that electrical stimulation of AC caused best frequencies in IC to shift towards the best frequencies of the stimulated site in AC (Gao & Suga, 1998, 2000; Ma & Suga, 2001b; J. Yan et al., 2005; W. Yan & Suga, 1998; X. Zhou & Jen, 2007). These results suggest that cortico-collicular feedback may be

important for increasing the representation of behaviorally relevant stimuli in IC. However, when activating direct feedback, we did not observe consistent changes in best frequency of IC neurons (**Figure 6D**). This may be due to activation of feedback projections across cortex, and therefore across the tonotopic map, in this paradigm.

Previous studies found no effect of activating projection terminals on responses in the CNIC, only shell regions of IC (Xiong et al., 2015), which are the predominant targets of cortico-collicular feedback. In our study we were able to record from a larger neuronal population, revealing a subset of neurons in central IC that were modulated by feedback. This is consistent with another study which observed enhanced white noise-induced activity in a small subset of neurons in the CNIC with activation of direct cortico-collicular feedback (Vila et al., 2019). The effects in central IC may be due to direct cortico-collicular feedback, intra-collicular circuits (Manuel S. Malmierca, Rees, Le Beau, & Bjaalie, 1995; Miller, Casseday, & Covey, 2005; Saldaña & Merchań, 1992; Sturm, Nguyen, & Kandler, 2014) , or a combination of these mechanisms.

Previous inactivation studies have shown mixed effects on sound-evoked responses in IC, but consistently demonstrated no effect on frequency selectivity, agreeing with our results. Specifically, suppression of AC increased or decreased IC sound responses in distinct subsets of cells (J Popelář et al., 2003; Jiří Popelář et al., 2016) while suppression of direct cortico-collicular feedback terminals in IC decreased sound-evoked responses (Xiong et al., 2015). It is possible that we saw little effect from suppression of cortico-collicular projections because inactivation through the auditory cortex suppressed only a subset of feedback projections to IC. Combined these studies suggest that at baseline, the cortex provides only weak modulation of IC activity.

Understanding how AC modulates sound responses in central IC may provide insight into how AC drives changes in auditory behavior. Previously, we found that behavioral frequency discrimination acuity changed after differential auditory fear conditioning and these changes were driven by the auditory cortex (Aizenberg & Geffen, 2013; Aizenberg et al., 2015). The behavioral task used to test frequency discrimination acuity was a modified pre-pulse inhibition (PPI) of the acoustic startle reflex task. Although AC can modulate this behavior, PPI is still observed after decerebration (Li & Frost, 2000) and the underlying circuit is believed to be subcortical (Fendt, Li, & Yeomans, 2001). The IC is a critical structure in the PPI circuit (Fendt et al., 2001; Leitner & Cohen, 1985; Li, Korngut, Frost, & Beninger, 1998), with the central nucleus of IC receiving ascending auditory projections and the external nucleus of IC acting as the output station (Fendt et al., 2001; Li & Yue, 2002). The broad frequency tuning in the shell regions of the IC (Barnstedt et al., 2015; Syka, Popelář, Kvašňák, & Astl, 2000) made the central nucleus of IC, which has sharper tuning and a tonotopic organization (Barnstedt et al., 2015; Ehret, Egorova, Hage, & Müller, 2003; M. S. Malmierca et al., 2008; Syka et al., 2000), a good candidate for how AC may drive changes in frequency discrimination acuity. Limited

evidence for a descending pathway from AC to the pedunculopontine tegmental nucleus (Schofield & Motts, 2009) suggests another alternative pathway by which AC modulates frequency discrimination.

We activated cortico-collicular neurons by shining light in the cortex, thus initiating spikes at the level of the cell body as would occur in response to a sound. An important consideration with this method, however, is that these neurons do not only send collaterals to IC, but also to the auditory thalamus (Asokan, Williamson, Hancock, & Polley, 2018; Williamson & Polley, 2019), amygdala (Asokan et al., 2018), and striatum (Asokan et al., 2018). There is also evidence of descending projections to IC from thalamus (Winer, Chernock, Larue, & Cheung, 2002) and amygdala (Marsh, Fuzessery, Grose, & Wenstrup, 2002). When interpreting our results it is important to consider that the effects we observe from activating cortico-collicular feedback may also be due, at least in part, to these secondary pathways. One caveat to consider in interpreting these results is that we used a square pulse for optogenetic manipulations, whereas a more complex stimulation pattern potentially can achieve stronger activation (Vila et al., 2019).

One caveat of our study is that our experiments were performed in passively listening mice. It is possible that the lack of effect we observe with suppression of cortico-collicular feedback is due to the lack of task engagement. Previous studies have found that inactivation of this pathway affects innate responses to sound (Xiong et al., 2015) and auditory learning (Bajo et al., 2010). Furthermore, studies have found that task engagement modulates neuronal responses to sounds (Downer, Rapone, Verhein, O'Connor, & Sutter, 2017; Fritz, Shamma, Elhilali, & Klein, 2003; Kuchibhotla et al., 2017; Lakatos et al., 2013; McGinley, David, & McCormick, 2015). Thus, we would expect suppression of this pathway to affect sound processing in IC during a behavioral task. Future studies should explore how activity changes with an animal actively engaged in a behavioral task.

We observed little effect of modulating AC inhibitory interneurons on activity in IC despite the changes observed in AC (**Figures 8, 9**), which suggests there may be another neuron subtype that plays a modulatory role during cortico-collicular plasticity in driving feedback modulation. One possibility that was not explored here are cholinergic inputs from the nucleus basalis. The nucleus basalis (NB), a cholinergic nucleus in the basal forebrain, has been implicated as a key structure in learning-induced auditory plasticity. Studies have found that pairing NB stimulation with presentation of a tone has been sufficient to induce receptive field plasticity in AC (Kilgard & Merzenich, 1998; Kilgard et al., 2001; Weinberger, 2003) and that blocking muscarinic receptors in AC impairs this plasticity (Miasnikov, Chen, & Weinberger, 2008). Of greater interest is the receptive field plasticity also observed in IC. Acetylcholine applied to AC increased spontaneous and tone-evoked activity in both AC and IC (Ji, Gao, & Suga, 2001). Furthermore, pairing AC stimulation with nucleus basalis stimulation (Ma & Suga, 2003) or pairing tone presentation with nucleus basalis stimulation (Zhang, Hakes, Bonfield, & Yan, 2005) shifted best frequencies in both AC and IC and application of atropine in AC inhibited this IC plasticity (Zhang et al., 2005). It is plausible that NB cholinergic inputs may be

355 responsible for driving responses of IC neurons rather than PV or SST inhibitory interneurons. However, SSTs
356 in AC are depolarized by application of cholinergic agonist (Kuchibhotla et al., 2017). While the lack of effect
357 we observe with interneuron inhibition might suggest that SST and PV interneurons are not involved in this
358 circuit, we must also consider that direct activation of feedback is not exactly equivalent to disinhibition. Direct
359 activation causes synchronized activation of cells, while disinhibition allows for asynchronous activation. This
360 difference may explain the different results. Furthermore, the lack of effect we observe with inhibitory
361 interneuron activation is consistent with our results from suppressing cortico-collicular feedback. Thus, while
362 another neuronal subtype may be responsible for driving feedback activity in a behavioral context, inhibitory
363 interneurons may still play a role in shaping responses of feedback once active.
364
365
366 **Materials and Methods**
367 **Animals.**
368 All experiments were performed in adult male and female mice (supplier: Jackson Laboratories; age, 12–15
369 wk; weight, 22–32 g; wild-type C57BL/6J RRID:IMSR_JAX:000664; *Pvalb-Cre* mice, strain: *B6;129P2-*
370 *Pvalbtm1(cre)Arbr/J* RRID:IMSR_JAX:008069; *Sst-Cre* mice, strain: *Ssttm2.1(cre)Zjh/J* RRID:IMSR_JAX:013044;
371 *Cdh23* mice, strain: *Cdh23tm2.1Kjn/J* RRID:IMSR_JAX:018399, or *Pvalb-Cre* x *Cdh23* or *Sst-Cre* x *Cdh23*
372 crosses). Mice were housed at 28°C on a 12 h light–dark cycle with water and food provided ad libitum, less
373 than five animals per cage. In *Pvalb-Cr*e mice Cre recombinase (Cre) was expressed in parvalbumin-positive
374 interneurons, and in *Sst-Cre*, Cre was expressed in somatostatin-positive interneurons. All animal work was
375 conducted according to the guidelines of University of Pennsylvanian IACUC (protocol number 803266) and
376 the AALAC Guide on Animal Research. Anesthesia by isoflurane and ketamine and euthanasia by CO2 were
377 used. All means were taken to minimize the pain or discomfort of the animals during and following the
378 experiments. All experiments were performed during the animals' dark cycle. Original spike data and code
379 are available on Dryad (https://datadryad.org/review?doi=doi:10.5061/dryad.1t61c80).
380
381 **Viral Vectors.**
382 Modified AAVs encoding ArchT (AAV9-CAG-FLEX-ArchT-GFP or AAV9-CAG-FLEX-ArchT-tdTomato;
383 UNC Vector Core) or ChR2 (AAV9-CAG-FLEX-ChR2-tdTomato; Penn Vector Core) were used for selective
384 suppression or excitation, respectively. Retrograde AAV virus encoding Cre (retro AAV-hSyn-Cre-GFP) was
385 custom made in our laboratory. Briefly, RetroAAV2 hSyn Cre-GFP was packaged using the Helper-Free
386 system (Agilent) and the retrograde trafficking plasmid, Retro2, which bears capsid mutations in serotype 2.
387

388 **Surgery and Virus Injection.**

389 At least 21 days prior to electrophysiological recordings, mice were anesthetized with isoflurane to a surgical
390 plane. The head was secured in a stereotactic holder. The mouse was subjected to a small craniotomy (2 x 2
391 mm) over AC under aseptic conditions. Viral particles were injected (750 nl) bilaterally using a syringe pump
392 (Pump 11 Elite, Harvard Apparatus) targeted to AC (coordinates relative to bregma: −2.6 mm anterior, ±4.3
393 mm lateral, +1 mm ventral). Fiber-optic cannulas (Thorlabs, Ø200 µm Core, 0.22 NA) were implanted
394 bilaterally over the injection site at depth of 0.5 mm from the skull surface. For a subset of mice, to target
395 direct feedback, the mouse was also subjected to a craniotomy over IC (1 x 4 mm). Retro AAV viral construct
396 was injected (3 x 200 nl) via glass syringe (30-50 um diameter) using a syringe pump (Pump 11 Elite, Harvard
397 Apparatus) bilaterally in IC. Craniotomies were covered with a removable silicon plug. A small headpost was
398 secured to the skull with dental cement (C&B Metabond) and acrylic (Lang Dental). For postoperative
399 analgesia, slow release Buprenex (0.1 mg/kg) and Bupivicane (2 mg/kg) were injected subcutaneously. An
400 antibiotic (5 mg/kg Baytril) was injected subcutaneously daily (for 4 days) at the surgical site during recovery.
401 Virus spread was confirmed in all mice postmortem by visualization of the fluorescent protein expression in
402 fixed brain tissue, and its colocalization with PV or SST or, for feedback cohort, expression in AC layer 5/6,
403 following immuno-histochemical processing with the appropriate antibody.

404 **Confocal Imaging.**

405 To confirm the location of viral injection sites, tissue sections containing the IC or AC were cut at 40 µm using
406 a cryostat. Sections were mounted onto glass slides and imaged using Zeiss LSM 800 confocal microscope.
407 20X images were taken throughout the entire IC or AC, and tiles were stitched together to form a composite
408 image using Zen software. Masks were drawn around the edge of the tissue to hide the embedding medium
409 using Photoshop.

410

411 **Acoustic Stimuli.**

412 Stimuli were delivered via a magnetic speaker (Tucker-Davis Technologies) directed toward the mouse's head.
413 Speakers were calibrated prior to the experiments to ±3 dB over frequencies between 3 and 70 kHz by placing
414 a microphone (Brüel and Kjaer) in the location of the ear contralateral to the recorded AC hemisphere,
415 recording speaker output and filtering stimuli to compensate for acoustic aberrations (Carruthers, Natan, &
416 Geffen, 2013). Free-standing speaker was used to approximate the conditions under which the mouse typically
417 experiences sounds in awake state.

418 *Clicks.*

419 To obtain a quick assessment of auditory onset responses we used click trains. Click trains were composed of
420 six 50 ms clicks at 70 dB sound pressure level relative to 20 microPascals (SPL) with a 50 ms ISI. Click trains

421 were repeated 120 times with a 450 ms ISI between trains. Alternating click trains were also paired with 1 s
422 laser stimulation beginning 250 ms prior to click train onset.
423 *Frequency tuning stimuli.*
424 (1) To measure tuning for direct feedback cohorts, a train of 50 pure tones of frequencies spaced
425 logarithmically between 3 and 70 kHz, at 70 dB SPL in pseudo-random order was presented 20 times. Each
426 tone was 50 ms duration (5-ms cosine squared ramp up and down) with an inter-stimulus interval (ISI) of
427 450 ms. Alternating tones were paired with continuous 250 ms laser pulse at either -100 ms, -20 ms, or +8 ms
428 onset relative to tone onset.
429 (2) For *Sst-Cre* and *Pvalb-Cre* cohorts, a train of pure tones of 35 frequencies spaced logarithmically between
430 3 and 70 kHz and 8 uniformly spaced intensities from 0 to 70 dB SPL were presented 10 times in a pseudo-
431 random order. Alternating tones were paired with continuous 250 ms laser pulse at -100 ms relative to tone
432 onset.
433 *Dynamic Random Chords (DRCs).*
434 To measure spectro-temporal receptive fields (STRFs) we constructed DRCs from 20 ms chords (with 1 ms
435 ramp) of 50 frequencies spaced logarithmically between 5 and 40 kHz with average intensity of 50 dB SPL
436 and 20 dB SPL standard deviation selected from a uniform distribution for each chord. Total duration was 40
437 minutes with a 250 ms continuous laser pulse presented every 1 s.
438
439 **Electrophysiological Recordings.**
440 All recordings were carried out inside a double-walled acoustic isolation booth (Industrial Acoustics). Mice
441 were placed in the recording chamber, and a headpost was secured to a custom base, immobilizing the head.
442 Activity of neurons in AC were recorded via a custom silicon multi-channel probe (Neuronexus), lowered in
443 the area targeting AC via a stereotactic instrument following a craniotomy at a 35-degree angle. The electrode
444 tips were arranged in a vertical fashion that permits recording the activity of neurons across the depth of the
445 auditory cortex and the inferior colliculus. Activity of neurons in IC were recorded via the same custom probes,
446 lowered in the area targeting IC via a stereotactic instrument following either a craniotomy (*Sst-Cre* and *Pvalb-*
447 *Cre* cohorts) or removal of the silicon plug, vertically. Recording sites in IC were identified based on
448 anatomical markers and stereotaxic coordinates as dorsal cortex (<0.5 mm of midline) or central nucleus of IC
449 (center of central nucleus of IC ~1 mm lateral of midline). Recordings were made in multiple locations across
450 IC. Electro-physiological data from 32 channels were filtered between 600 and 6000 Hz (spike responses),
451 digitized at 32kHz and stored for offline analysis (Neuralynx). Spikes belonging to single neurons and multi-
452 units were detected using commercial software (Plexon). Original spike data and code are available on Dryad
453 (https://datadryad.org/review?doi=doi:10.5061/dryad.1t61c80). We examined the experimental groups
454 described in ***Table 1*** (note: we do not distinguish here between *Sst-Cre*/ *Pvalb-Cre* and *Sst-Cre* x *Cdh23* and

455 *Pvalb-Cre* x *Cdh23*). Initial experiments were performed under anesthesia to control for stability or recordings.
456 For cohorts with awake and anesthetized recordings data were analyzed separately, but we observed no
457 difference in our results so data were combined (**Figure 8 – figure supplement 1**). We used power analysis
458 for effect size of 25% and expected variance in firing rate (50%) to determine the minimum total number of
459 units for each experimental group at N=44. All groups included a greater number of units (single- and multi-
460 units were combined in analysis). The number of units in measuring tone-evoked responses are specified in
461 ***Table 1***. Mice that did not show effect of laser activation or suppression in auditory cortex were excluded. We
462 recorded from AC in Cdh23+ChR2 mice and Cdh23+ArchT mice to verify an effect in AC (**Figure 3- figure**
463 **supplement 2**) in all mice used in our analysis.
464

Group	Recording Area	Single Units	Multi Units	Awake Total Mice	Awake Total Units	Anesthetized Total Mice	Anesthetized Total Units	Total Units
Cdh23-ChR2	IC	4	187	5 Male	191	-	-	191
Cdh23-ArchT	IC	24	181	4 Male	205	-	-	205
PV-ChR2	IC	25	198	4 Male	85	12 Male	138	223
	AC	3	64		14		53	67
PV-ArchT	IC	6	40	4 Male	46	-	-	46
	AC	3	56		59		-	59
SST-ChR2	IC	15	90	7 Male	76	8 Male	29	105
	AC	9	90		49		50	99
SST-ArchT	IC	16	161	2 Male	140	4 Male	37	177
	AC	4	155	2 Female	123	2 Female	36	159

465
466 ***Table 1.*** Number of recorded units and mice used in our analyses for each experimental group and condition.
467
468 **Photostimulation of Neuronal Activity.**
469 Neurons were stimulated by application of continuous light pulse delivered from either blue (473 nm,
470 BL473T3-150, used for ChR2 stimulation) or green DPSS laser (532 nm, GL532T3-300, Slocs lasers, used
471 for ArchT stimulation) through implanted cannulas. Laser power measured through cannulas was 3 mW.
472 Timing of the light pulse was controlled with microsecond precision via a custom control shutter system,
473 synchronized to the acoustic stimulus delivery.
474
475 **Neural Response Analysis.**
476 *Unit selection.* Units were selected based on pure-tone responsiveness. For each unit we identified the 7
477 frequencies that elicited the highest response and averaged activity across these trials (and the highest 3
478 amplitudes for stimulus with multiple amplitudes). Units with tone-evoked activity (75 ms window after tone
479 onset) less than two standard deviations above the spontaneous activity (50 ms window prior to tone onset) in
480 no laser condition were excluded from the analysis. Both single units and high quality multi-units (multi-units
481 with <1% of spikes with <1ms inter-spike-interval) were used.

Spontaneous activity and tone-evoked response magnitude. Feedback cohort: Spontaneous activity was the average firing rate in a 20 ms window (to allow for equivalent comparison between -100 ms and -20 ms laser onset conditions) prior to tone onset of top 7 preferred frequencies.

Sst-Cre/Pvalb-Cre cohorts: Spontaneous activity was the average firing rate in a 50 ms window prior to tone onset of top 7 preferred frequencies and 3 highest amplitudes.

All mice: Tone-evoked response magnitude was calculated as the difference between the average tone-evoked response in a 75 ms window after tone onset and the spontaneous activity.

Sparseness. To examine frequency selectivity of neurons, sparseness of frequency tuning was computed as:

$$Sparseness = 1 - \frac{\left(\sum_{i=1}^{i=n} \frac{FR_i}{n}\right)^2}{\sum_{i=1}^{i=n} \frac{FR_i^2}{n}}$$

where FR_i is tone-evoked firing rate response to tone at frequency i, and n is number of frequencies used (Weliky, Fiser, Hunt, & Wagner, 2003). Subgroups of neurons used in sparseness analyses were separated based on changes in spontaneous activity or tone-evoked response magnitude in response to cortico-collicular activation or suppression. Units were selected if > 1 standard deviation change in spontaneous activity or tone-evoked response magnitude based on the -100 ms laser onset trials.

Linear fits across frequencies. Linear fits were calculated using linear regression (fitlm.m; MATLAB) over 50 data points, one for each of the 50 frequencies tested (Natan, Rao, & Geffen, 2017). The 50 data points were separately calculated as the mean FR over all repeats of each frequency.

Best Frequency. Best frequency was defined as the frequency that elicited the maximum response.

STRF Analysis. To calculate the STRF we separated the stimulus into 1-second chunks, concatenating the 250 ms laser ON chunks and the 250 ms laser OFF chunks immediately preceding laser onset. These data were then used to calculate the average spectrogram preceding a spike. To allow for finer temporal resolution of the STRFs we upsampled the DRCs using nearest neighbor interpolation. Subsequently we averaged the STRF across the eight stimulus files. To determine the significance of the lobes, the *z*-score of pixels was computed relative to the baseline values from an STRF generated with scrambled spike trains, using Stat4ci toolbox (Chauvin, Worsley, Schyns, Arguin, & Gosselin, 2005; Natan, Carruthers, Mwilambwe-Tshilobo, & Geffen, 2017). We ran this significance test 100 times and any pixel identified as significant more than 90 times was considered significant. Lobes were matched between laser ON and laser OFF trials by comparing the overlap of the lobes, requiring a 50% overlap of the smallest lobe size to be a match. From the STRF, the peak time, temporal width, peak frequency, and frequency width of the positive and negative lobes were measured (Schneider & Woolley, 2010; Shechter & Depireux, 2007; Woolley, Gill, & Theunissen, 2006).

Noise Correlation.

Noise correlations were calculated as the pairwise Pearson correlation coefficient between the spike counts of units recorded simultaneously. For spontaneous activity spikes were counted in a window 20 ms before tone onset and for tone response spikes were counted in a window 75 ms after tone onset.

Statistical Analyses.

Significant differences and *P* values were calculated using paired Wilcoxon sign-rank test (unless noted otherwise) with standard MATLAB routine. For the laser alone data, to compare distributions to standard normal distribution data were normalized by mean and standard deviation and then significant differences and *P* values were calculated by Kolmogorov-Smirnoff test with standard MATLAB routine. Mean ± standard error of the mean was reported unless stated otherwise. * indicates $p < 0.05$, ** indicates $p < 0.01$, *** indicates $p < 0.001$.

Acknowledgements. This work was supported by National Institutes of Health (Grant numbers NIH R03DC013660, NIH R01DC014779, NIH R01DC015527), Klingenstein Award in Neuroscience, Human Frontier in Science Foundation Young Investigator Award and the Pennsylvania Lions Club Hearing Research Fellowship to MNG. MNG is the recipient of the Burroughs Wellcome Award at the Scientific Interface. JMB was supported by NIH T32MH017168. We thank the members of the Geffen laboratory and the Hearing Research Center at the University of Pennsylvania, including Dr. Steve Eliades and Dr. Yale Cohen for comments on an earlier version of the manuscript. We also thank Sarah Kwon for assistance with confocal imaging.

Competing interests: The authors declare that no competing interests exist.

Figure 1

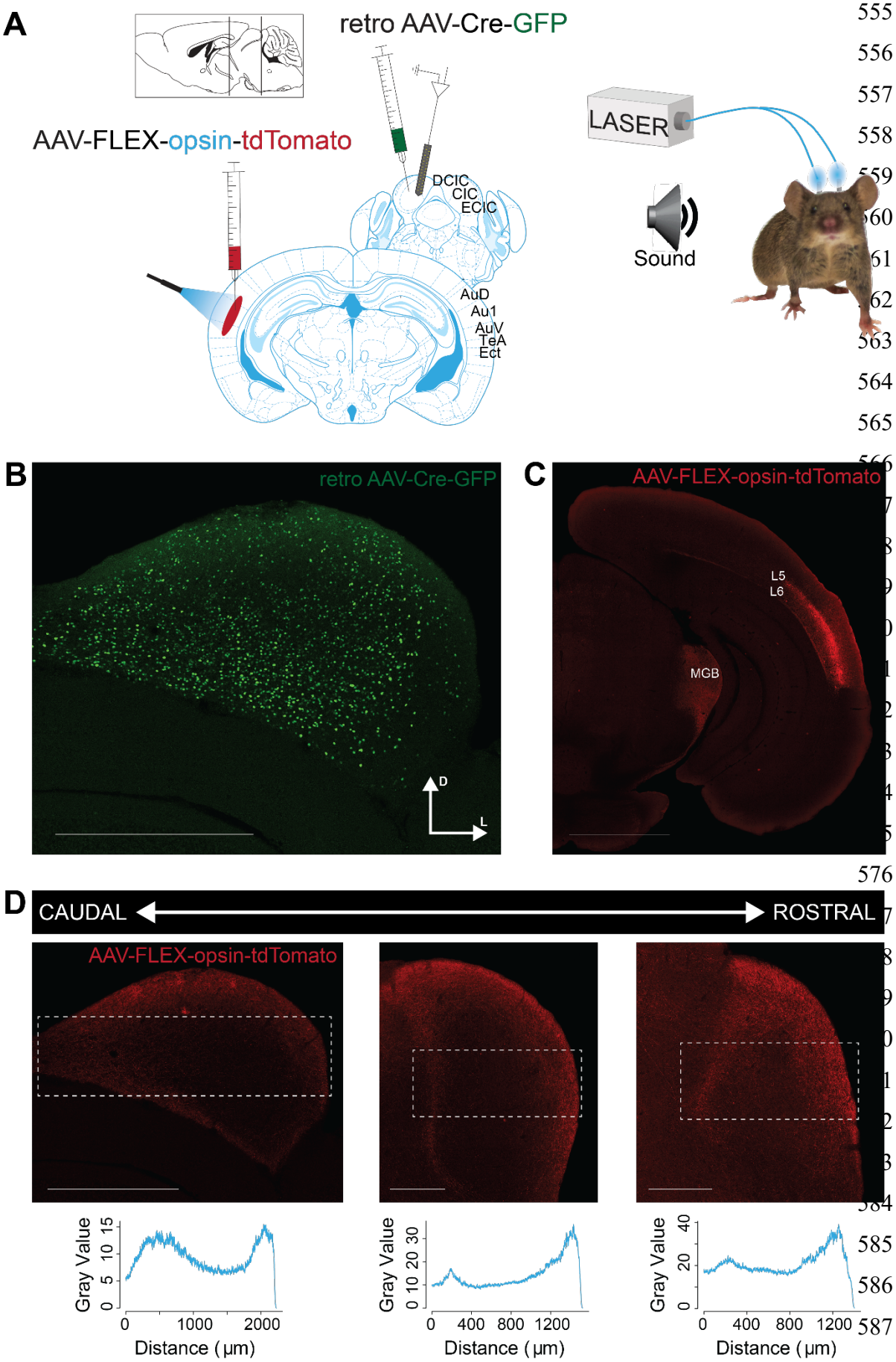
A
retro AAV-Cre-GFP
AAV-FLEX-opsin-tdTomato
DCIC
CIC
ECIC
AuD
Au1
AuV
TeA
Ect
LASER
Sound
B
retro AAV-Cre-GFP
D
L
C
AAV-FLEX-opsin-tdTomato
L5
L6
MGB
D
CAUDAL
ROSTRAL
AAV-FLEX-opsin-tdTomato
Gray Value
Distance (μm)
0
1000
2000
400
800
1200

588 **Figure 1.** Opsin expression in corticocollicular feedback. **A** Experimental design: To yield selective labeling
589 of auditory cortico-collicular projections, a retro AAV-Cre-GFP construct is injected into the IC and an
590 anterograde AAV-FLEX-opsin-tdTomato construct is injected into the AC. Recordings are made in multiple
591 bilateral locations of the IC (left) of awake mice. Cannulas are implanted bilaterally in the auditory cortex, and
592 a green/blue laser is used to silence/activate the cortico-collicular pathway (right). **B** Expression of the retro
593 AAV-Cre-GFP construct in the IC. Scale bar: 1000 µm. **C** Selective expression of the AAV-FLEX-opsin-
594 tdTomato construct in cell bodies in layer 5 (L5) and 6 (L6) of the AC that project to the IC. Fiber and terminal
595 labeling is also present in the medial geniculate body, a known target of auditory cortico-collicular cells. Scale
596 bar: 2000 µm. **D** Expression of the AAV-FLEX-opsin-tdTomato construct in fibers and terminals at multiple
597 rostro-cadual levels of the IC. Expression, as measured by fluorescence intensity (bottom), is strongest in
598 medial portions of the central nucleus of the IC and lateral portions of the external nucleus of the IC. Scale
599 bar: left, 1000 µm; middle and right, 500 µm.
600
601
602
603

Figure 2

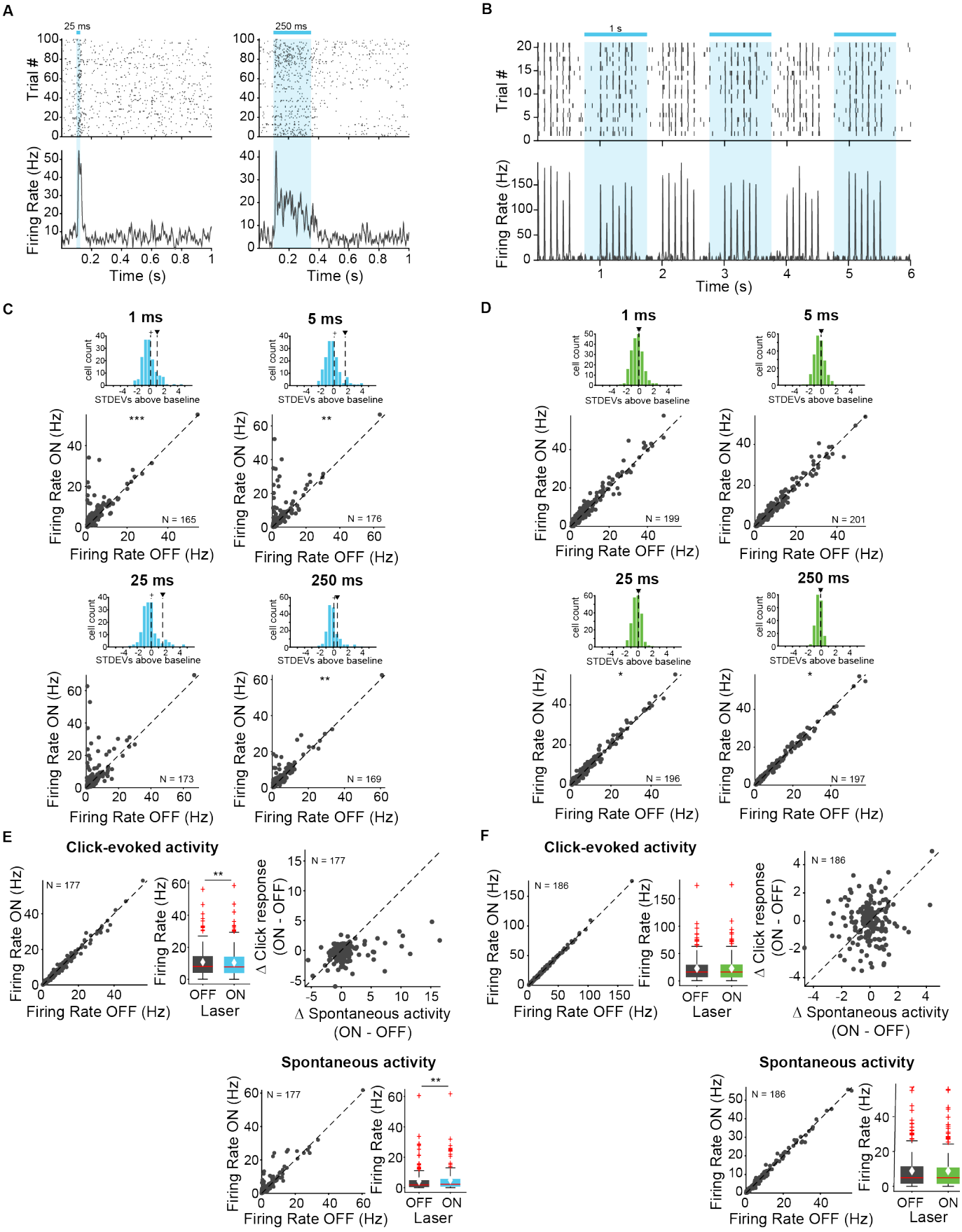
A
25 ms
250 ms
Trial #
Firing Rate (Hz)
Time (s)
B
1 s
Trial #
Firing Rate (Hz)
Time (s)
C
1 ms
5 ms
25 ms
250 ms
cell count
STDEVs above baseline
Firing Rate ON (Hz)
Firing Rate OFF (Hz)
N = 165
N = 176
N = 173
N = 169
D
1 ms
5 ms
25 ms
250 ms
N = 199
N = 201
N = 196
N = 197
E
Click-evoked activity
N = 177
Firing Rate ON (Hz)
Firing Rate OFF (Hz)
Firing Rate (Hz)
OFF
ON
Laser
Δ Click response (ON - OFF)
Δ Spontaneous activity (ON - OFF)
Spontaneous activity
F
Click-evoked activity
N = 186
Spontaneous activity

604

605 **Figure 2**. Effects of modulating feedback activity on firing rate in IC in the absence of sounds and to clicks.
606 **A** Example unit response to two laser pulse durations (blue), 25 ms (left) and 250 ms (right). **B** Example unit
607 response to clicks with (blue) and without laser. **C** Change in unit activity in response to different laser
608 durations in ChR2 cohort (1 ms, 5 ms, 25 ms, 250 ms). *Top panel*: Distribution of changes in unit activity, +
609 indicates median, ▼ indicates mean. These distributions are not normally distributed (Kolmogorov-Smirnov
610 test; *1 ms*: p = 3.07e-15, mean = 1.1 stdevs, median = 0.21 stdevs; *5 ms*: p = 4.4e-20, mean = 1.7 stdevs, median
611 = 0.19 stdevs; *25 ms*: p = 5.5e-17, mean = 1.6 stdevs, median = -0.021 stdevs; *250 ms*: p = 3.4e-12, mean =
612 0.58 stdevs, median = 0.101 stdevs). *Bottom panel*: Population changes in unit activity (*1 ms*: p = 5.3e-4, ON
613 = 5.6 ± 0.6 Hz, OFF = 4.9 ± 0.5 Hz; *5 ms*: p = 0.0027, ON = 6.9 ± 0.7 Hz, OFF = 4.8 ± 0.5 Hz; *250 ms*: p =
614 0.005, ON = 5.6 ± 0.6 Hz, OFF = 4.8 ± 0.5 Hz)). **D** Change in unit activity in response to different laser
615 durations in ArchT cohort (1 ms, 5 ms, 25 ms, 250 ms). *Top panel:* Distribution of changes in unit activity, +
616 indicates median, ▼ indicates mean. These distributions are normally distributed (Kolmogorov-Smirnov test).
617 Bottom panel: Population changes in unit activity (2*5 ms*: p = 0.039, ON = 9.5 ± 0.7 Hz, OFF = 9.5 ± 0.7 Hz;
618 *250 ms*: p = 0.02, ON = 9.5 ± 0.8 Hz, OFF = 9.5 ± 0.8 Hz). **E** Population response to clicks with activation
619 shows a decrease in click response (left; p = 0.001, click ON = 10.4 ± 1.2 Hz, click OFF = 10.7 ± 1.1 Hz) and
620 an increase in spontaneous activity (bottom; p = 0.0031, spont ON = 5 ± 0.87 Hz, spont OFF = 4.3 ± 0.92 Hz).
621 On box plots, red line indicates median, white ◆ indicates mean. **F** Population response to clicks with
622 suppression shows no change in activity. On box plots, red line indicates median, white ◆ indicates mean.
623
624
625
626
627
628
629
630
631
632
633
634
635
636
637
638

Figure 3

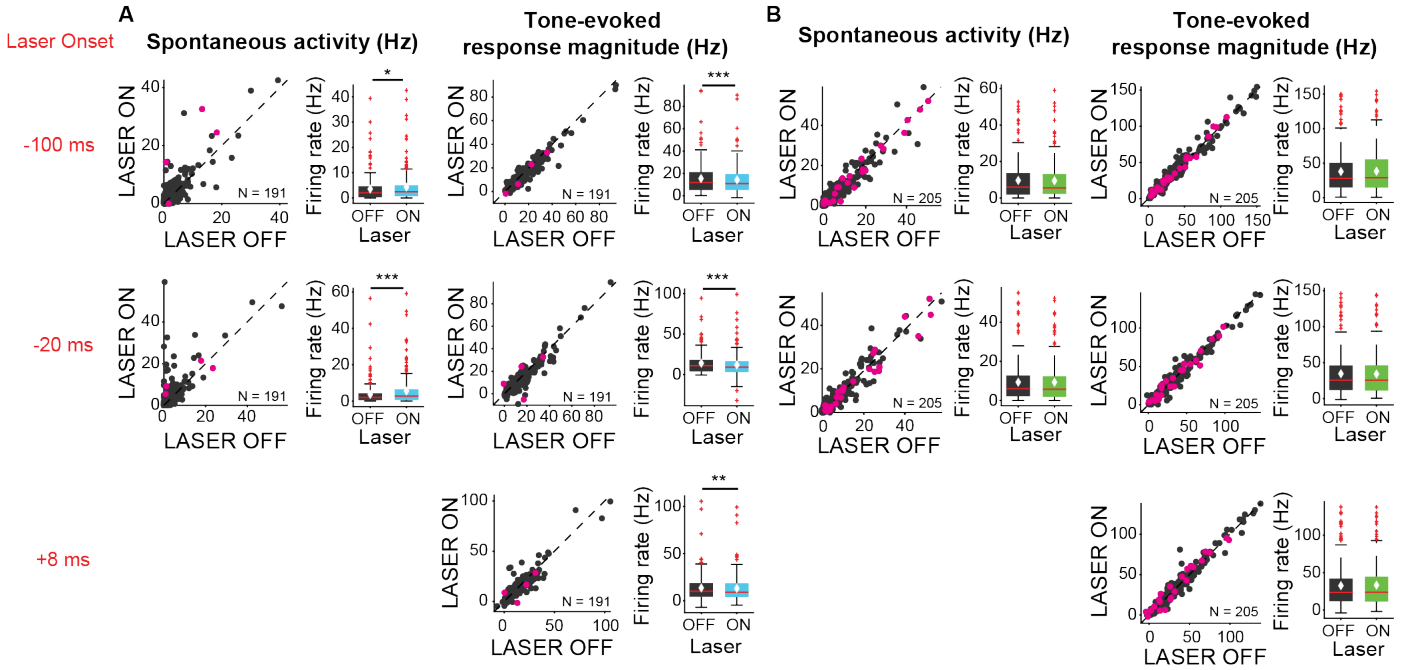

Figure 3. Effects of modulating feedback activity on spontaneous and tone-evoked response magnitude in IC. Left panels: neuronal activity (spontaneous, left or tone-evoked, right) on laser on versus laser off trials. Right panels: Average neuronal activity (spontaneous, left or tone-evoked, right) for laser on and laser off trials. Magenta circles indicate single units. On box plots, red line indicates median, white ◆ indicates mean. **A** Activating feedback increased spontaneous activity (left; *-100 ms*: p = 0.022, ON = 4.3 ± 0.47 Hz; OFF = 3.6 ± 0.38; *-20 ms*: p = 8.6e-6, ON = 5.6 ± 0.63, OFF = 3.7 ± 0.47) and decreased tone-evoked response magnitude (right; *-100 ms*: p = 3.2e-5, ON = 14.2 ± 0.98 Hz; OFF = 15.5 ± 1.04 Hz; *-20 ms*: p = 1.4e-6, ON = 11.8 ± 1.08 Hz, OFF = 13.9 ± 1 Hz; *+8 ms*: p = 0.0034, ON = 13.03 ± 1.03, OFF = 13.7 ± 1.03). **B** Suppressing feedback had no effect on spontaneous activity or tone-evoked response magnitude.

Figure 4

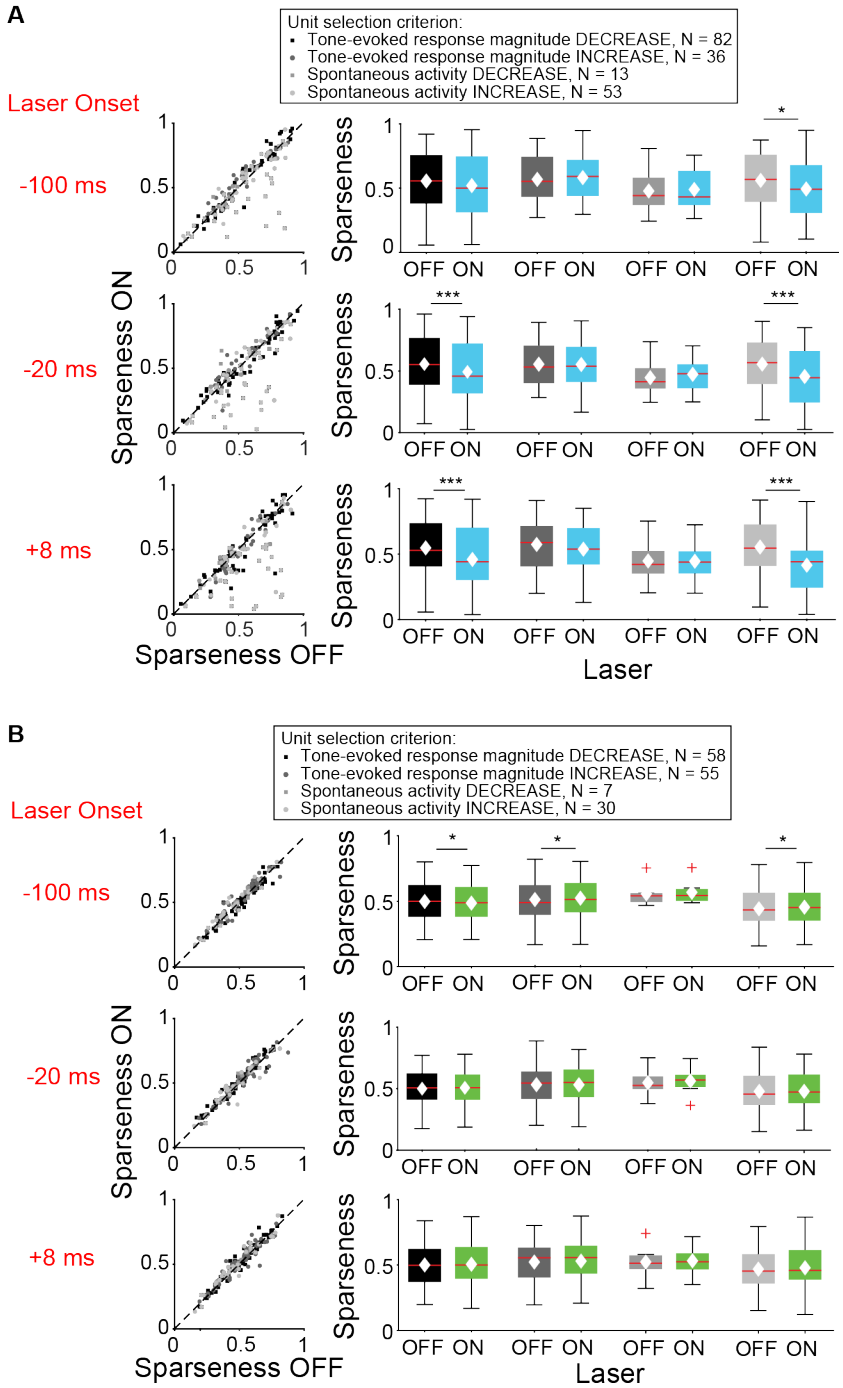

Figure 4. Effect of modulating direct cortico-collicular feedback at different latencies relative to tone onset on frequency selectivity in IC. On box plots, red line indicates median, white ◆ indicates mean. **A** Left panels: Sparseness for laser on versus laser off trials. Right panels: Average sparseness for laser on and laser off trials. Activating feedback decreased frequency selectivity in a subset of units (mag decrease: *-20 ms*, p = 0.00031, sparse ON = 0.49 ± 0.027, sparse OFF = 0.55 ± 0.025; *+8 ms*, p = 0.00029, sparse ON = 0.46 ± 0.027, sparse OFF = 0.55 ± 0.024; spont increase: *-100 ms*, p = 0.011, sparse ON = 0.49 ± 0.032, sparse OFF = 0.56 ± 0.031; *-20 ms*, p = 0.00018, sparse ON = 0.46 ± 0.034, sparse OFF = 0.56 ± 0.029; *+8 ms*, p = 2.2e-6, sparse ON =

0.41 ± 0.032, sparse OFF = 0.55 ± 0.029). **B** Left panels: Sparseness for laser on versus laser off trials. Right panels: Average sparseness for laser on and laser off trials. Suppressing feedback has little effect on frequency selectivity (mag decrease: -100 ms, p = 0.011, sparse ON = 0.53 ± 0.021, sparse OFF = 0.51 ± 0.021; mag increase: -100 ms, p = 0.019, sparse ON = 0.48 ± 0.021, sparse OFF = 0.49 ± 0.021; spont increase: -100 ms, p = 0.043, sparse ON = 0.46 ± 0.029, sparse OFF = 0.45 ± 0.029).

Figure 5

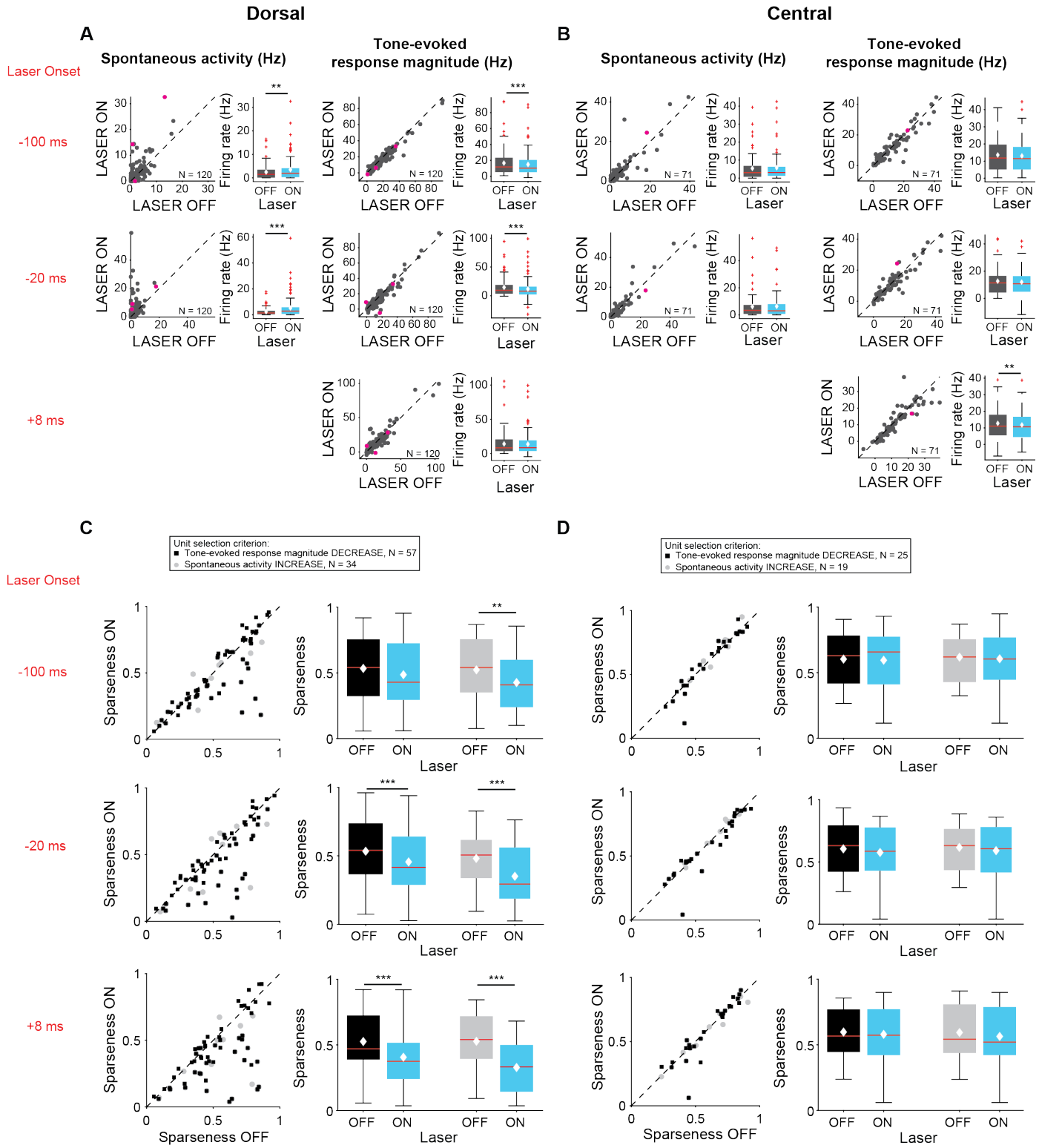

Figure 5. Effects of activating cortico-collicular feedback on responses in IC for CNIC (A,C) and DCIC (B,D) recording sites. On box plots, red line indicates median, white ◆ indicates mean. **A** Increase in spontaneous activity (left; *-100 ms*: p = 0.0204, ON = 3.5 ± 0.5 Hz, OFF = 2.5 ± 0.3 Hz; *-20 ms*: p = 2.8e-7, ON = 5.2 ± 0.7 Hz, OFF = 2.3 ± 0.3 Hz) and decrease in tone-evoked response magnitude (right, *-100 ms*: p

= 3.3e-6, ON = 14.8 ± 1.4 Hz, OFF = 16.5 ± 1.5 Hz; *-20 ms*: p = 6.3e-7, ON = 11.8 ± 1.6 Hz, OFF = 14.7 ± 1.4 Hz) for cells in DCIC. Left panels: neuronal activity (spontaneous, left or tone-evoked, right) on laser on versus laser off trials. Right panels: Average neuronal activity (spontaneous, left or tone-evoked, right) for laser on and laser off trials. **B** Little change in spontaneous activity or tone-evoked response magnitude (right; +8 ms: p = 0.0027, ON = 13 ± 1.2 Hz, OFF = 13.6 ± 1.2 Hz) for cells in CNIC. **C** Left panels: Sparseness for laser on versus laser off trials. Right panels: Average sparseness for laser on and laser off trials. Activating feedback decreases frequency selectivity in a subset of units (mag decrease: *-20 ms*, p = 6.3e-4, sparse ON = 0.46 ± 0.03, sparse OFF = 0.53 ± 0.03; *+8 ms*, p = 4.7e-5, sparse ON = 0.41 ± 0.03, sparse OFF = 0.53 ± 0.03; spont increase: *-100 ms*, p = 0.0044, sparse ON = 0.43 ± 0.04, sparse OFF = 0.52 ± 0.04; *-20 ms*, p = 0.00013, sparse ON = 0.39 ± 0.04, sparse OFF = 0.53 ± 0.04; *+8 ms*, p = 5.2e-6, sparse ON = 0.33 ± 0.03, OFF = 0.53 ± 0.04) for cells in DCIC. **D** Activating feedback has no effect on frequency selectivity of cells in CNIC.

Figure 6

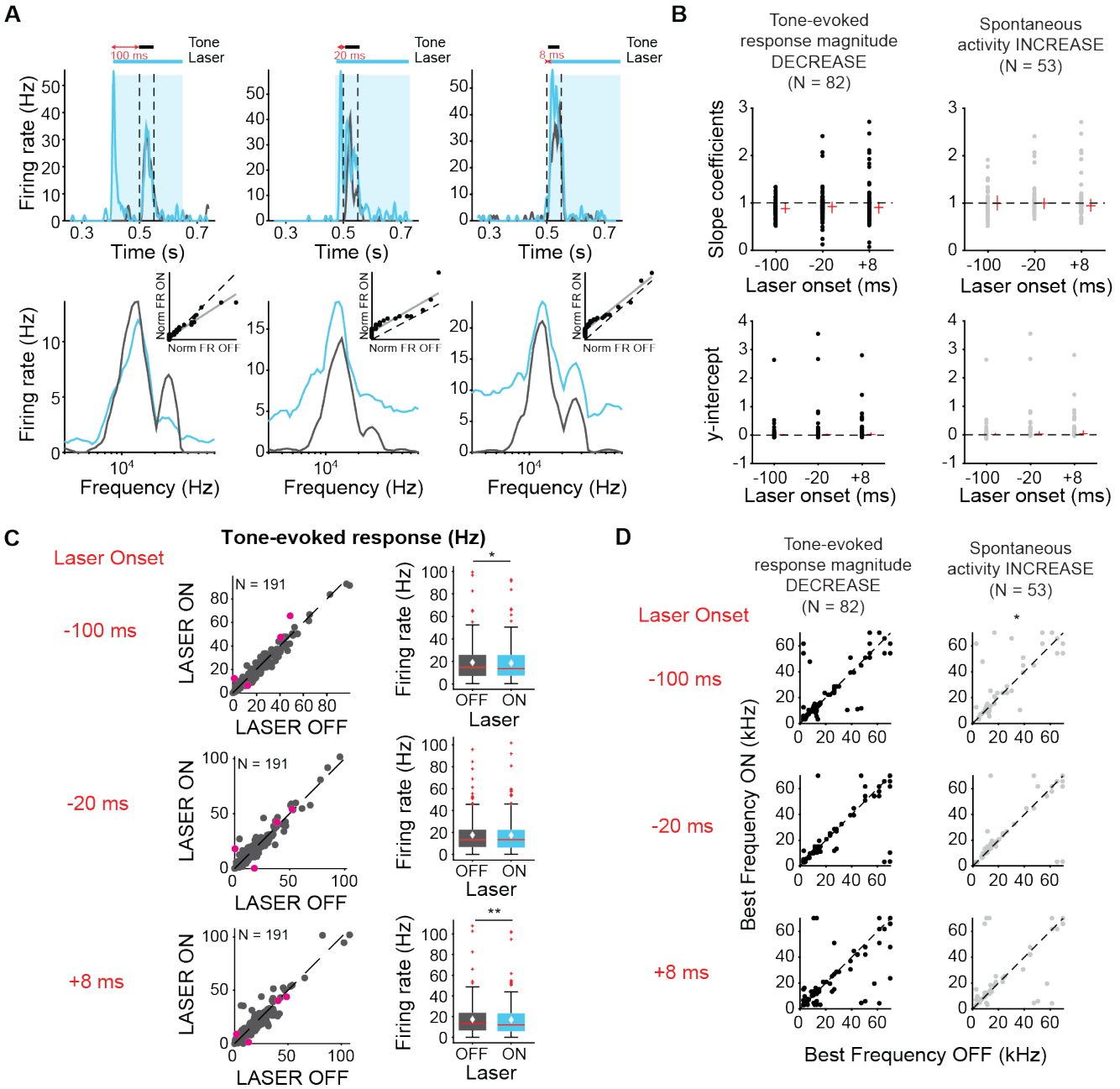

Figure 6. A Example unit response timecourse (top) and tuning curves (bottom) for laser on (blue) and laser off (grey) conditions. Bottom insets represent ranked linear fits for example unit. **B** Slope coefficients (top, mag decrease: *-100 ms*, median = 0.88; *-20 ms*, median = 0.92; *+8 ms*, median = 0.903; spont increase: *-100 ms*, median = 0.99; *-20 ms*, median = 1; *+8 ms*, median = 0.94) and y-intercepts (bottom, mag decrease: *-100 ms*, median = 0.0086; *-20 ms*, median = 0.014; *+8 ms*, median = 0.022; spont increase: *-100 ms*, median = 0.014; *-20 ms*, median = 0.025; *+8 ms*, median = 0.037) of ranked linear fits, red horizontal lines indicate median, red vertical lines indicate interquartile range. **C** Left panels: Tone-evoked response for laser on versus laser off trials. Magenta circles indicate single units. Right panels: Average tone-evoked response for laser on

and laser off trials. On box plots, red line indicates median, white ◆ indicates mean. Activating feedback slightly decreased tone-evoked response, averaged across 7 most preferred frequencies (-*100ms*: p = 0.018, ON = 19.01 ± 1.2 Hz, OFF = 18.5 ± 1.2 Hz; +*8ms*: p = 0.007, ON = 17.3 ± 1.2 Hz; OFF = 16.9 ± 1.2 Hz) **D** Best frequencies for laser off versus laser on trials. Activating feedback had little effect on best frequency (spont increase: -*100 ms*, p = 0.022).

Figure 7

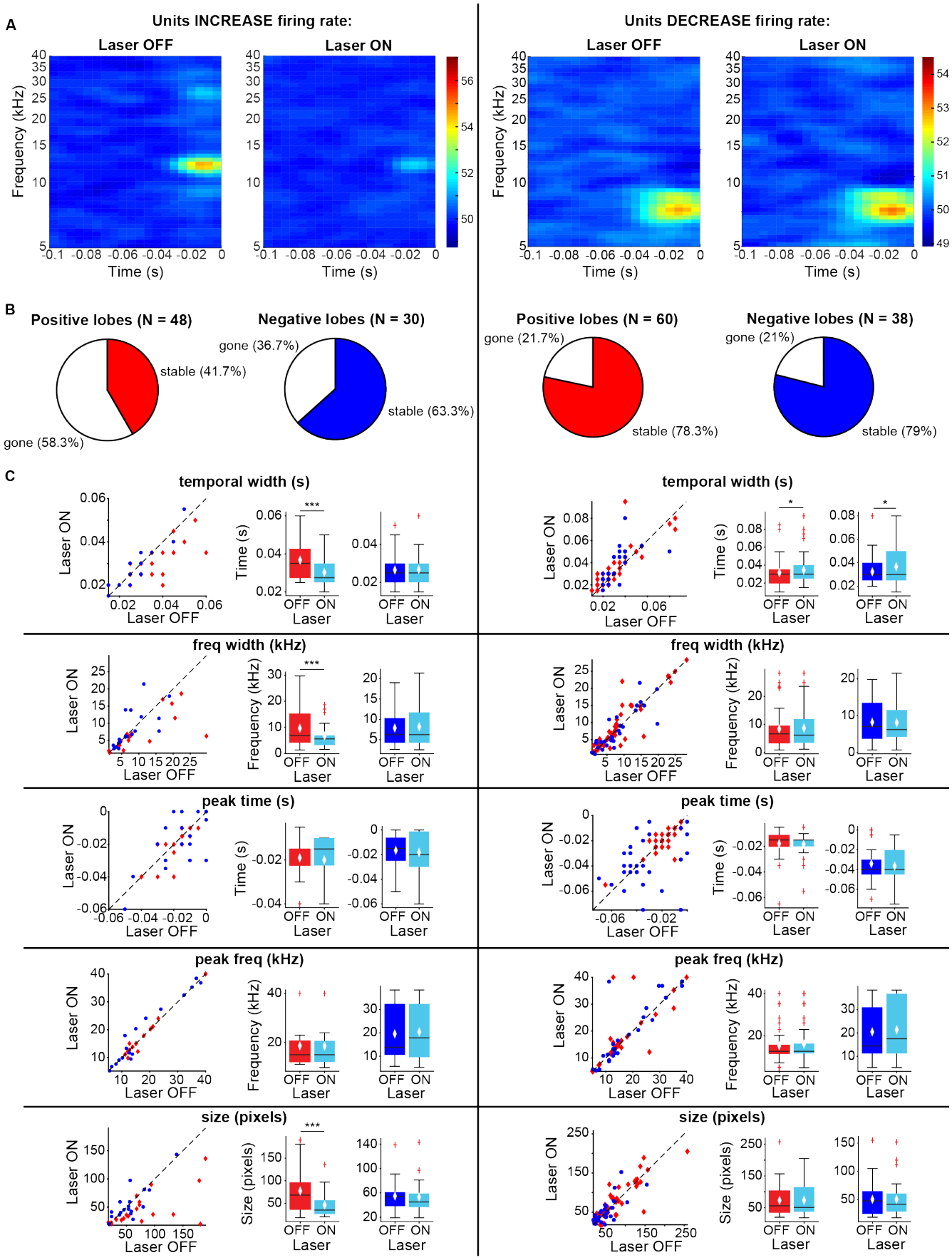
A
Units INCREASE firing rate:
Laser OFF
Laser ON
Units DECREASE firing rate:
Frequency (kHz)
Time (s)
B
Positive lobes (N = 48)
Negative lobes (N = 30)
Positive lobes (N = 60)
Negative lobes (N = 38)
gone (58.3%)
stable (41.7%)
gone (36.7%)
stable (63.3%)
gone (21.7%)
stable (78.3%)
gone (21%)
stable (79%)
C
temporal width (s)
freq width (kHz)
peak time (s)
peak freq (kHz)
size (pixels)
Laser ON
Laser OFF
Time (s)
Frequency (kHz)
Size (pixels)
OFF ON
Laser

Figure 7. Effects of activating direct cortico-collicular feedback on STRF properties. **A** Example STRF with and without activation of feedback for units that increase firing rate (left) and decrease firing rate (right) in response to feedback activation. **B** Number of positive and negative lobes that persisted with laser (stable). **C** Changes in STRF parameters of stable positive and negative lobes. Left panels: STRF parameter for laser off versus laser on trials. Center panels: Average positive lobe STRF parameter for laser on and laser off trials. Right panels: Average negative lobe STRF parameter for laser on and laser off trials. On box plots, red line indicates median, white ◆ indicates mean. For units with an increase in firing rate we observed a decrease in temporal width ($p = 0.00098$, ON = 0.0303 ± 0.0018 s, OFF = 0.037 ± 0.0023 s), frequency width ($p = 0.00042$, ON = 6.7 ± 1.1 Hz, OFF = 9.6 ± 1.8 Hz), and overall size ($p = 0.00036$, ON = 46.05 ± 6.9 pixels, OFF = 77.5 ± 12.04 pixels) of positive lobes. For units with a decrease in firing rate we observed only a small increase in temporal width for both positive ($p = 0.026$, ON = 0.034 ±0.0025 s, OFF = 0.032 ± 0.0025 s) and negative ($p = 0.02$, ON = 0.037 ± 0.0028 s, OFF = 0.032 ± 0.0024 s) lobes.

Figure 8

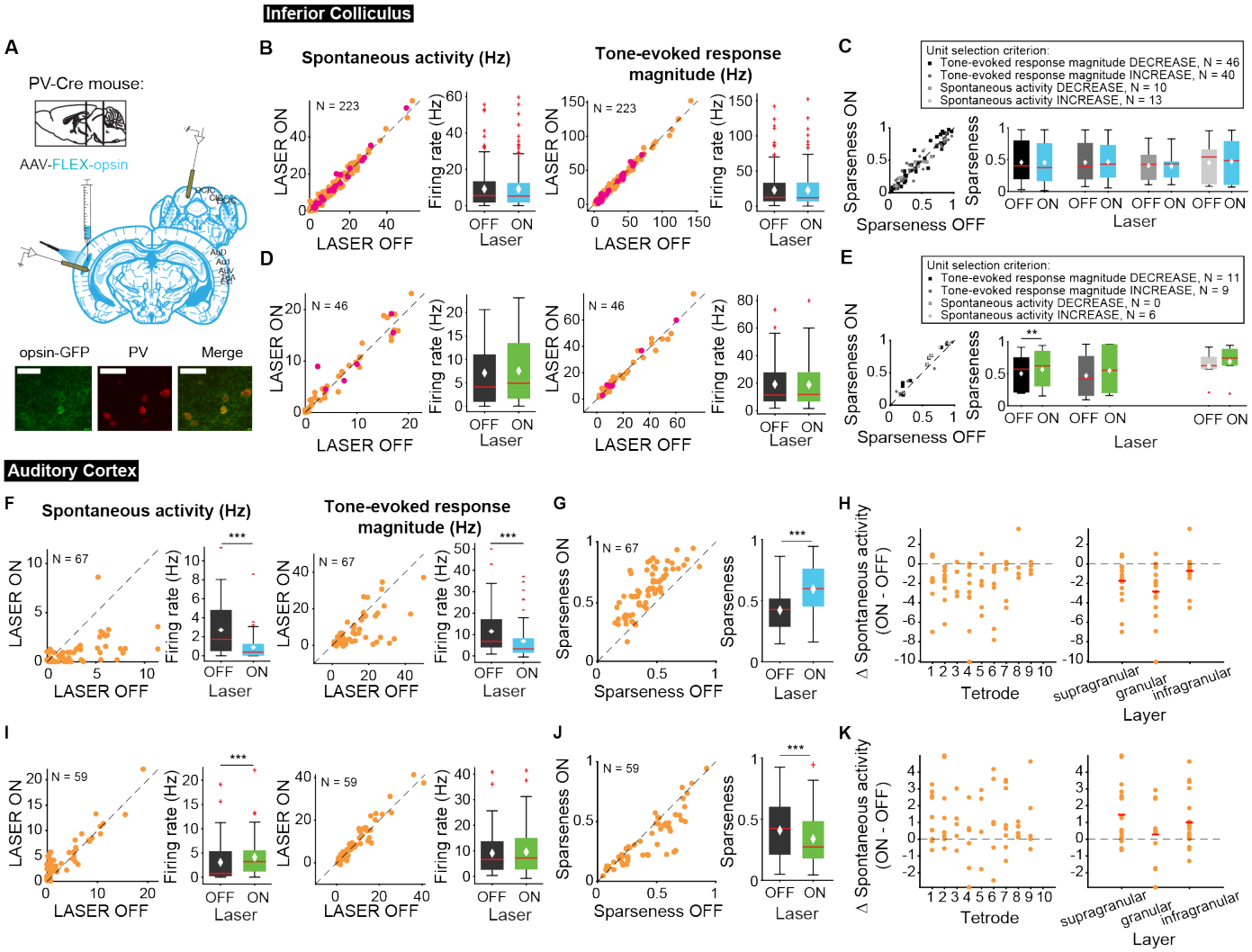

Figure 8. Effects of modulating PV interneurons in AC on tone-evoked responses in IC. On box plots, red line indicates median, white ◆ indicates mean. **A** Stain for PV (center) and opsin-GFP (left). Scale bar: 50um. **B** Activating PVs had no effect on spontaneous activity or tone-evoked response magnitude in IC. Magenta circles indicate single units. **C** Activating PVs had no effect on frequency selectivity in IC. **D** Suppressing PVs had no effect on spontaneous activity or tone-evoked response magnitude in IC. Magenta circles indicate single units. **E** Suppressing PVs had weak effects on frequency selectivity in IC (mag decrease: p = 0.0068, ON = 0.57 ± 0.092, OFF = 0.5 ± 0.087). **F** Activating PVs decreased spontaneous activity (p = 2.2e-9, ON = 0.88 ± 0.16 Hz, OFF = 2.7 ± 0.34 Hz) and tone-evoked response magnitude (p = 8.02e-7, ON = 6.9 ± 1.06 Hz, OFF = 11.5 ± 1.3 Hz) in AC. **G** Activating PVs increased frequency selectivity in putative excitatory units in AC (p = 3.3e-12, ON = 0.59 ± 0.022, OFF = 0.42 ± 0.02). **H** Activating PVs affected putative excitatory units across all layers of AC. **I** Suppressing PVs increased spontaneous activity (p = 5.2e-5, ON = 4.08 ± 0.54 Hz, OFF = 3.06 ± 0.55 Hz) but does not affect tone-evoked response magnitude in AC. **J** Suppressing PVs decreased frequency selectivity in AC (p = 3.8e-5, ON = 0.34 ± 0.027, OFF = 0.41 ± 0.031). **K** Suppressing

PVs affected putative excitatory units across all layers of AC. **B,D,F,I** Left panels: neuronal activity (spontaneous, left or tone-evoked, right) on laser on versus laser off trials. Right panels: Average neuronal activity (spontaneous, left or tone-evoked, right) for laser on and laser off trials. **C,E,G,J** Left panels: Sparseness for laser on versus laser off trials. Right panels: Average sparseness for laser on and laser off trials. **H,K** Change in spontaneous activity (laser on trials – laser off trials), left panels: for units at each tetrode; right panels: separated into supragranular: tetrodes 1-3; granular: tetrodes 5,6; infragranular: tetrodes 7-10.

Figure 9

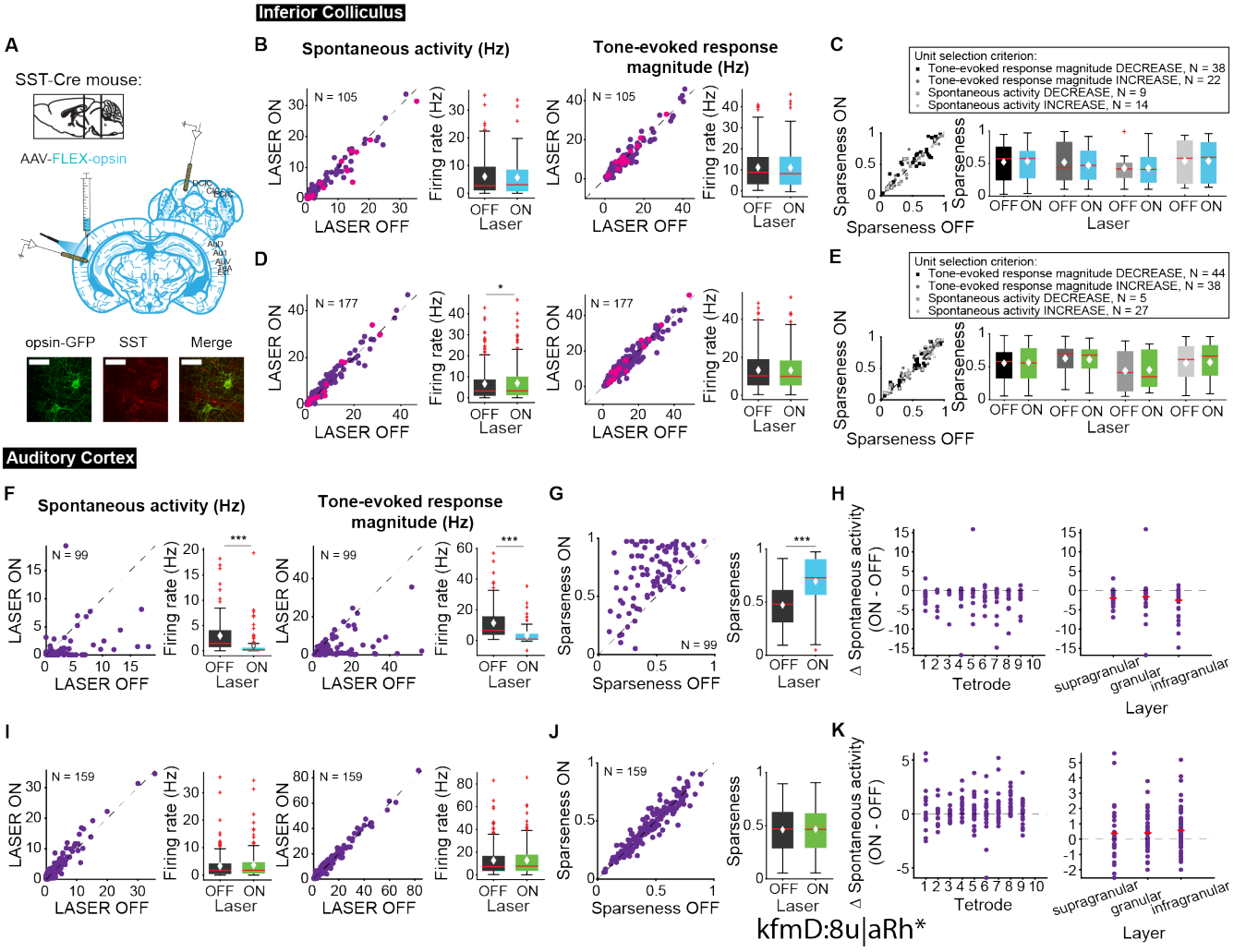

Figure 9. Effects of modulating SST interneurons in AC on tone-evoked responses in IC. On box plots, red line indicates median, white ◆ indicates mean. **A** Stain for SST (center) and opsin-GFP (left). Scale bar: 50um. **B** Activating SSTs had no effect on spontaneous activity or tone-evoked response magnitude in IC. Magenta circles indicate single units. **C** Activating SSTs had no effect on frequency selectivity in IC. **D** Suppressing SSTs increased spontaneous activity (p = 0.029, ON = 6.9 ± 0.66 Hz, OFF = 6.7 ± 0.63 Hz) but did not affect tone-evoked response magnitude in IC. Magenta circles indicate single units. **E** Suppressing SSTs had no effect on frequency selectivity in IC. **F** Activating SSTs decreased spontaneous activity (p = 1.4e-12, ON = 0.97 ± 0.25 Hz, OFF = 2.9 ± 0.37 Hz) and tone-evoked response magnitude (p = 1.3e-15, ON = 3.3 ± 0.59 Hz, OFF = 11.4 ± 1.2 Hz) in AC. **G** Activating SSTs increased frequency selectivity in putative excitatory units in AC (p = 1.6e-13, ON = 0.69 ± 0.024, OFF = 0.47 ± 0.019). **H** Activating SSTs affected putative excitatory units across all layers of AC. **I** Suppressing SSTs increased spontaneous activity (p = 8.1e-4, ON = 3.6 ± 0.41 Hz, OFF = 2.2 ± 0.38 Hz) but did not affect tone-evoked response magnitude in AC. **J** Suppressing SSTs had no effect on frequency selectivity in AC. **K** Suppressing SSTs affected putative excitatory units across all layers of AC. **B,D,F,I** Left panels: neuronal activity (spontaneous, left or tone-evoked, right) on laser on versus laser off trials. Right panels: Average neuronal activity (spontaneous, left or tone-evoked, right) for laser on

and laser off trials. **C,E,G,J** Left panels: Sparseness for laser on versus laser off trials. Right panels: Average sparseness for laser on and laser off trials. **H,K** Change in spontaneous activity (laser on trials – laser off trials), left panels: for units at each tetrode; right panels: separated into supragranular: tetrodes 1-3; granular: tetrodes 5,6; infragranular: tetrodes 7-10.

References

Abbott, L. F., & Dayan, P. (1999). The Effect of Correlated Variability on the Accuracy of a Population Code. *Neural Computation*, *11*(1), 91–101. doi: 10.1162/089976699300016827

Aizenberg, M., & Geffen, M. N. (2013). Bidirectional effects of aversive learning on perceptual acuity are mediated by the sensory cortex. *Nature Neuroscience*, *16*(8), 994–996. doi: 10.1038/nn.3443

Aizenberg, M., Mwilambwe-Tshilobo, L., Briguglio, J. J., Natan, R. G., & Geffen, M. N. (2015). Bidirectional Regulation of Innate and Learned Behaviors That Rely on Frequency Discrimination by Cortical Inhibitory Neurons. *PLoS Biology*, *13*(12), 1–32. doi: 10.1371/journal.pbio.1002308

Alitto, H. J., & Usrey, W. M. (2003). Corticothalamic feedback and sensory processing. *Current Opinion in Neurobiology*, *13*(4), 440–445. doi: 10.1016/S0959-4388(03)00096-5

Asokan, M. M., Williamson, R. S., Hancock, K. E., & Polley, D. B. (2018). Sensory overamplification in layer 5 auditory corticofugal projection neurons following cochlear nerve synaptic damage. *Nature Communications*, *9*(1), 2468. doi: 10.1038/s41467-018-04852-y

Averbeck, B. B., Latham, P. E., & Pouget, A. (2006). Neural correlations, population coding and computation. *Nature Reviews Neuroscience*, *7*, 358–366. doi: 10.1038/nrn1888

Bajo, V. M., & Moore, D. R. (2005). Descending projections from the auditory cortex to the inferior colliculus in the gerbil, Meriones unguiculatus. *The Journal of Comparative Neurology*, *486*, 101–116. doi: 10.1002/cne.20542

Bajo, V. M., Nodal, F. R., Bizley, J. K., Moore, D. R., & King, a. J. (2007). The Ferret Auditory Cortex: Descending Projections to the Inferior Colliculus. *Cerebral Cortex*, *17*(2), 475–491. doi: 10.1093/cercor/bhj164

Bajo, V. M., Nodal, F. R., Moore, D. R., & King, A. J. (2010). The descending corticocollicular pathway mediates learning-induced auditory plasticity. *Nature Neuroscience*, *13*(2), 253–260. doi: 10.1038/nn.2466

Barnstedt, O., Keating, P., Weissenberger, Y., King, A. J., & Dahmen, J. C. (2015). Functional Microarchitecture of the Mouse Dorsal Inferior Colliculus Revealed through In Vivo Two-Photon Calcium Imaging. *The Journal of Neuroscience : The Official Journal of the Society for Neuroscience*,

35(31), 10927–10939. doi: 10.1523/JNEUROSCI.0103-15.2015

Carruthers, I. M., Natan, R. G., & Geffen, M. N. (2013). Encoding of ultrasonic vocalizations in the auditory cortex. *Journal of Neurophysiology*, *109*, 1912–1927. doi: 10.1152/jn.00483.2012

Chauvin, A., Worsley, K. J., Schyns, P. G., Arguin, M., & Gosselin, F. (2005). Accurate statistical tests for smooth classification images. *Journal of Vision*, *5*, 659–667. doi: 10.1167/5.9.1

Coomes, D. L., Schofield, R. M., & Schofield, B. R. (2005). Unilateral and bilateral projections from cortical cells to the inferior colliculus in guinea pigs. *Brain Research*, *1042*, 62–72. doi: 10.1016/J.BRAINRES.2005.02.015

Doucet, J. R., Molavi, D. L., & Ryugo, D. K. (2003). The source of corticocollicular and corticobulbar projections in area Te1 of the rat. *Experimental Brain Research*, *153*, 461–466. doi: 10.1007/s00221-003-1604-4

Downer, J. D., Rapone, B., Verhein, J., O'Connor, K. N., & Sutter, M. L. (2017). Feature-Selective Attention Adaptively Shifts Noise Correlations in Primary Auditory Cortex. *The Journal of Neuroscience : The Official Journal of the Society for Neuroscience*, *37*(21), 5378–5392. doi: 10.1523/JNEUROSCI.3169-16.2017

Ehret, G., Egorova, M., Hage, S. R., & Müller, B. A. (2003). Spatial map of frequency tuning-curve shapes in the mouse inferior colliculus. *NeuroReport*, *14*(10), 1365–1369. doi: 10.1097/00001756-200307180-00017

Feliciano, M., & Potashner, S. J. (1995). Evidence for a Glutamatergic Pathway from the Guinea Pig Auditory Cortex to the Inferior Colliculus. *Journal of Neurochemistry*, *65*(3), 1348–1357.

Fendt, M., Li, L., & Yeomans, J. S. (2001). Brain stem circuits mediating prepusle inhibition of the startle reflex. *Psychopharmacology*, *156*, 216–224. doi: 10.1007/s002130100794

Fritz, J., Shamma, S., Elhilali, M., & Klein, D. (2003). Rapid task-related plasticity of spectrotemporal receptive fields in primary auditory cortex. *Nature Neuroscience*, *6*(11), 1216–1223. doi: 10.1038/nn1141

Gao, E., & Suga, N. (1998). Experience-dependent corticofugal adjustment of midbrain frequency map in bat auditory system. *PNAS*, *95*, 12663–12670.

Gao, E., & Suga, N. (2000). Experience-dependent plasticity in the auditory cortex and the inferior colliculus of bats : Role of the corticofugal system. *PNAS*, *97*(14), 8081–8086.

Hamilton, L. S., Sohl-Dickstein, J., Huth, A. G., Carels, V. M., Deisseroth, K., & Bao, S. (2013). Optogenetic activation of an inhibitory network enhances feedforward functional connectivity in auditory cortex. *Neuron*, *80*(4), 1066–1076. doi: 10.1016/j.neuron.2013.08.017

Jen, P. H.-S., Chen, Q. C., & Sun, X. D. (1998). Corticofugal regulation of auditory sensitivity in the bat inferior colliculus. *Journal of Comparative Physiology A*, *183*, 683–697.

Jen, P. H.-S., & Zhou, X. (2003). Corticofugal modulation of amplitude domain processing in the midbrain of the big brown bat, Eptesicus fuscus. *Hearing Research*, *184*, 91–106. doi: 10.1016/S0378-5955(03)00237-5

Ji, W., Gao, E., & Suga, N. (2001). Effects of Acetylcholine and Atropine on Plasticity of Central Auditory Neurons Caused by Conditioning in Bats. *Journal of Neurophysiology*, *86*(1), 211–225. doi: 10.1152/jn.2001.86.1.211

Kilgard, M. P., & Merzenich, M. M. (1998). Cortical Map Reorganization Enabled by Nucleus Basalis Activity. *Science*, *279*, 1714–1718. doi: 10.1126/science.279.5357.1714

Kilgard, M. P., Pandya, P. K., Vazquez, J., Gehi, A., Schreiner, C. E., & Merzenich, M. M. (2001). Sensory Input Directs Spatial and Temporal Plasticity in Primary Auditory Cortex. *Journal of Neurophysiology*, *86*(1), 326–338. doi: 10.1152/jn.2001.86.1.326

Kuchibhotla, K. V, Gill, J. V, Lindsay, G. W., Papadoyannis, E. S., Field, R. E., Sten, T. A. H., … Froemke, R. C. (2017). Parallel processing by cortical inhibition enables context-dependent behavior. *Nature Neuroscience*, *20*, 62–71. doi: 10.1038/nn.4436

Lakatos, P., Musacchia, G., O'Connel, M. N., Falchier, A. Y., Javitt, D. C., & Schroeder, C. E. (2013). The spectrotemporal filter mechanism of auditory selective attention. *Neuron*, *77*(4), 750–761. doi: 10.1016/j.neuron.2012.11.034

Leitner, D. S., & Cohen, M. E. (1985). Role of the inferior colliculus in the inhibition of acoustic startle in the rat. *Physiology & Behavior*, *34*, 65–70. doi: 10.1016/0031-9384(85)90079-4

Li, L., & Frost, B. J. (2000). Azimuthal directional sensitivity of prepulse inhibition of the pinna startle reflex in decerebrate rats. *Brain Research Bulletin*, *51*(1), 95–100. doi: 10.1016/S0361-9230(99)00215-4

Li, L., Korngut, L. M., Frost, B. J., & Beninger, R. J. (1998). Prepulse inhibition following lesions of the inferior colliculus: prepulse intensity functions. *Physiology & Behavior*, *65*(1), 133–139. doi: 10.1016/S0031-9384(98)00143-7

Li, L., & Yue, Q. (2002). Auditory gating processes and binaural inhibition in the inferior colliculus. *Hearing Research*, *168*, 98–109. doi: 10.1016/S0378-5955(02)00356-8

Lim, H. H., & Anderson, D. J. (2007). Antidromic Activation Reveals Tonotopically Organized Projections From Primary Auditory Cortex to the Central Nucleus of the Inferior Colliculus in Guinea Pig. *Journal of Neurophysiology*, *97*, 1413–1427. doi: 10.1152/jn.00384.2006

Ma, X., & Suga, N. (2001a). Corticofugal modulation of duration-tuned neurons in the midbrain auditory nucleus in bats. *PNAS*, *98*(24), 14060–14065.

Ma, X., & Suga, N. (2001b). Plasticity of Bat's Central Auditory System Evoked by Focal Electric Stimulation of Auditory and/or Somatosensory Cortices. *Journal of Neurophysiology*, *85*(3), 1078–

1087.

Ma, X., & Suga, N. (2003). Augmentation of Plasticity of the Central Auditory System by the Basal Forebrain and/or Somatosensory Cortex. *Journal of Neurophysiology*, *89*, 90–103. doi: 10.1152/jn.00968.2001

Malmierca, M. S., Izquierdo, M. A., Cristaudo, S., Hernandez, O., Perez-Gonzalez, D., Covey, E., & Oliver, D. L. (2008). A Discontinuous Tonotopic Organization in the Inferior Colliculus of the Rat. *Journal of Neuroscience*, *28*(18), 4767–4776. doi: 10.1523/JNEUROSCI.0238-08.2008

Malmierca, Manuel S., Rees, A., Le Beau, F. E. N., & Bjaalie, J. G. (1995). Laminar organization of frequency-defined local axons within and between the inferior colliculi of the guinea pig. *The Journal of Comparative Neurology*, *357*(1), 124–144. doi: 10.1002/cne.903570112

Markovitz, C. D., Tang, T. T., & Lim, H. H. (2013). Tonotopic and localized pathways from primary auditory cortex to the central nucleus of the inferior colliculus. *Frontiers in Neural Circuits*, *7*, 1–11. doi: 10.3389/fncir.2013.00077

Marsh, R. A., Fuzessery, Z. M., Grose, C. D., & Wenstrup, J. J. (2002). Projection to the Inferior Colliculus from the Basal Nucleus of the Amygdala. *Journal of Neuroscience*, *22*(23), 10449–10460. doi: 10.1523/JNEUROSCI.22-23-10449.2002

McGinley, M. J., David, S. V, & McCormick, D. A. (2015). Cortical Membrane Potential Signature of Optimal States for Sensory Signal Detection. *Neuron*, *87*(1), 179–192. doi: 10.1016/j.neuron.2015.05.038

Miasnikov, A. A., Chen, J. C., & Weinberger, N. M. (2008). Specific auditory memory induced by nucleus basalis stimulation depends on intrinsic acetylcholine. *Neurobiology of Learning and Memory*, *90*(2), 443–454. doi: 10.1016/j.nlm.2008.05.010

Miller, K. E., Casseday, J. H., & Covey, E. (2005). Relation between intrinsic connections and isofrequency contours in the inferior colliculus of the big brown bat, Eptesicus fuscus. *Neuroscience*, *136*(3), 895–905. doi: 10.1016/J.NEUROSCIENCE.2005.04.032

Natan, R. G., Carruthers, I. M., Mwilambwe-Tshilobo, L., & Geffen, M. N. (2017). Gain Control in the Auditory Cortex Evoked by Changing Temporal Correlation of Sounds. *Cerebral Cortex*, *27*, 2385–2402. doi: 10.1093/cercor/bhw083

Natan, R. G., Rao, W., & Geffen, M. N. (2017). Cortical Interneurons Differentially Shape Frequency Tuning following Adaptation. *Cell Reports*, *21*, 878–890. doi: 10.1016/J.CELREP.2017.10.012

Nirenberg, S., & Latham, P. E. (2003). Decoding neuronal spike trains: How important are correlations? *PNAS*, *100*(12), 7348–7353.

Phillips, E. A., & Hasenstaub, A. R. (2016). Asymmetric effects of activating and inactivating cortical interneurons. *ELife*, *5*, 1–22. doi: 10.7554/elife.18383

Popelář, J, Nwabueze-Ogbo, F. C., & Syka, J. (2003). Changes in Neuronal Activity of the Inferior Colliculus in Rat after Temporal Inactivation of the Auditory Cortex. *Physiol. Res*, *52*, 615–628.

Popelář, Jiří, Šuta, D., Lindovský, J., Bureš, Z., Pysanenko, K., Chumak, T., & Syka, J. (2016). Cooling of the auditory cortex modifies neuronal activity in the inferior colliculus in rats. *Hearing Research*, *332*, 7–16. doi: 10.1016/j.heares.2015.10.021

Rouiller, E. M., & Durif, C. (2004). The dual pattern of corticothalamic projection of the primary auditory cortex in macaque monkey. *Neuroscience Letters*, *358*, 49–52. doi: 10.1016/J.NEULET.2004.01.008

Rudy, B., Fishell, G., Lee, S., & Hjerling-Leffler, J. (2011). Three groups of interneurons account for nearly 100% of neocortical GABAergic neurons. *Developmental Neurobiology*, *71*(1), 45–61. doi: 10.1002/dneu.20853

Saldaña, E., Feliciano, M., & Mugnaini, E. (1996). Distribution of descending projections from primary auditory neocortex to inferior colliculus mimics the topography of intracollicular projections. *The Journal of Comparative Neurology*, *371*(1), 15–40. doi: 10.1002/(SICI)1096-9861(19960715)371:1<15::AID-CNE2>3.0.CO;2-O

Saldaña, E., & Merchań, M. A. (1992). Intrinsic and commissural connections of the rat inferior colliculus. *Journal of Comparative Neurology*, *319*(3), 417–437. doi: 10.1002/cne.903190308

Schneider, D. M., & Woolley, S. M. N. (2010). Discrimination of Communication Vocalizations by Single Neurons and Groups of Neurons in the Auditory Midbrain. *Journal of Neurophysiology*, *103*(6), 3248–3265. doi: 10.1152/jn.01131.2009

Schofield, B. R., & Motts, S. D. (2009). Projections from auditory cortex to cholinergic cells in the midbrain tegmentum of guinea pigs. *Brain Research Bulletin*, *80*(3), 163–170. doi: 10.1016/J.BRAINRESBULL.2009.06.015

Seybold, B. A., Elizabeth, A. K., Schreiner, C. E., Hasenstaub, A. R., Seybold, B. A., Phillips, E. A. K., … Hasenstaub, A. R. (2015). Inhibitory Actions Unified by Network Integration Viewpoint Inhibitory Actions Unified by Network Integration. *Neuron*, *87*(6), 1181–1192. doi: 10.1016/j.neuron.2015.09.013

Shadlen, M. N., & Newsome, W. T. (1998). The variable discharge of cortical neurons: implications for connectivity, computation, and information coding. *The Journal of Neuroscience*, *18*(10), 3870–3896. doi: 10.1523/JNEUROSCI.18-10-03870.1998

Shechter, B., & Depireux, D. A. (2007). Stability of spectro-temporal tuning over several seconds in primary auditory cortex of the awake ferret. *Neuroscience*, *148*(3), 806–814. doi: 10.1016/j.neuroscience.2007.06.027

Straka, M. M., Hughes, R., Lee, P., & Lim, H. H. (2015). Descending and tonotopic projection patterns from the auditory cortex to the inferior colliculus. *Neuroscience*, *300*, 325–337. doi: 10.1016/J.NEUROSCIENCE.2015.05.032

Sturm, J., Nguyen, T., & Kandler, K. (2014). Development of intrinsic connectivity in the central nucleus of the mouse inferior colliculus. *The Journal of Neuroscience : The Official Journal of the Society for Neuroscience*, *34*(45), 15032–15046. doi: 10.1523/JNEUROSCI.2276-14.2014

Syka, J., Popelář, J., Kvašňák, E., & Astl, J. (2000). Response properties of neurons in the central nucleus and external and dorsal cortices of the inferior colliculus in guinea pig. *Experimental Brain Research*, *133*, 254–266. doi: 10.1007/s002210000426

Vila, C. H., Williamson, R. S., Hancock, K. E., & Polley, D. B. (2019). Optimizing optogenetic stimulation protocols in auditory corticofugal neurons based on closed-loop spike feedback. *Journal of Neural Engineering*, *16*(6), 066023. doi: 10.1088/1741-2552/ab39cf

Weinberger, N. M. (2003). The nucleus basalis and memory codes: Auditory cortical plasticity and the induction of specific, associative behavioral memory. *Neurobiology of Learning and Memory*, *80*(3), 268–284. doi: 10.1016/S1074-7427(03)00072-8

Weliky, M., Fiser, J., Hunt, R. H., & Wagner, D. N. (2003). Coding of Natural Scenes in Primary Visual Cortex. *Neuron*, *37*, 703–718. doi: 10.1016/S0896-6273(03)00022-9

Williamson, R. S., & Polley, D. B. (2019). Parallel systems for sound processing and functional connectivity among layer 5 and 6 auditory corticothalamic neurons. *BioRxiv*, *doi*, 10.1101/447276. doi: 10.1101/447276

Winer, J. A., Chernock, M. L., Larue, D. T., & Cheung, S. W. (2002). Descending projections to the inferior colliculus from the posterior thalamus and the auditory cortex in rat, cat, and monkey. *Hearing Research*, *168*, 181–195. doi: 10.1016/S0378-5955(02)00489-6

Winer, J. A., Diehl, J. J., & Larue, D. T. (2001). Projections of auditory cortex to the medial geniculate body of the cat. *The Journal of Comparative Neurology*, *430*, 27–55. doi: 10.1002/1096-9861(20010129)430:1<27::AID-CNE1013>3.0.CO;2-8

Winer, J. A., Larue, D. T., Diehl, J. J., & Hefti, B. J. (1998). Auditory cortical projections to the cat inferior colliculus. *The Journal of Comparative Neurology*, *400*(2), 147–174. doi: 10.1002/(SICI)1096-9861(19981019)400:2<147::AID-CNE1>3.0.CO;2-9

Wood, K. C., Blackwell, J. M., & Geffen, M. N. (2017). Cortical inhibitory interneurons control sensory processing. *Current Opinion in Neurobiology*, *46*, 200–207. doi: 10.1016/J.CONB.2017.08.018

Woolley, S. M. N., Gill, P. R., & Theunissen, F. E. (2006). Stimulus-Dependent Auditory Tuning Results in Synchronous Population Coding of Vocalizations in the Songbird Midbrain. *Journal of Neuroscience*, *26*(9), 2499–2512. doi: 10.1523/jneurosci.3731-05.2006

Xiong, X. R., Liang, F., Zingg, B., Ji, X., Ibrahim, L. A., Tao, H. W., & Zhang, L. I. (2015). Auditory cortex controls sound-driven innate defense behaviour through corticofugal projections to inferior colliculus. *Nature Communications*, *6*, 7224. doi: 10.1038/ncomms8224

Yan, J., Zhang, Y., Ehret, G., & Yan, J. (2005). Corticofugal shaping of frequency tuning curves in the central nucleus of the inferior colliculus of mice. *J Neurophysiol*, *93*, 71–83. doi: 10.1152/jn.00348.2004

Yan, W., & Suga, N. (1998). Corticofugal modulation of the midbrain frequency map in the bat. *Nature Neuroscience*, *1*(1), 54–58.

Zhang, Y., Hakes, J. J., Bonfield, S. P., & Yan, J. (2005). Corticofugal feedback for auditory midbrain plasticity elicited by tones and electrical stimulation of basal forebrain in mice. *European Journal of Neuroscience*, *22*(4), 871–879. doi: 10.1111/j.1460-9568.2005.04276.x

Zhang, Y., Suga, N., & Yan, J. (1997). Corticofugal modulation of frequency processing in bat auditory system. *Nature*, *387*(June), 900–903.

Zhou, X., & Jen, P. H.-S. (2007). Corticofugal Modulation of Multi-Parametric Auditory Selectivity in the Midbrain of the Big Brown Bat. *Journal of Neurophysiology*, *98*(5), 2509–2516. doi: 10.1152/jn.00613.2007

Zhou, Xiaoming, & Jen, P. H.-S. (2005). Corticofugal modulation of directional sensitivity in the midbrain of the big brown bat, Eptesicus fuscus. *Hearing Research*, *203*, 201–215. doi: 10.1016/j.heares.2004.12.008

Zohary, E., Shadlen, M. N., & Newsome, W. T. (1994). Correlated neuronal discharge rate and its implications for psychophysical performance. *Nature*, *370*, 140–143. doi: 10.1038/370140a0

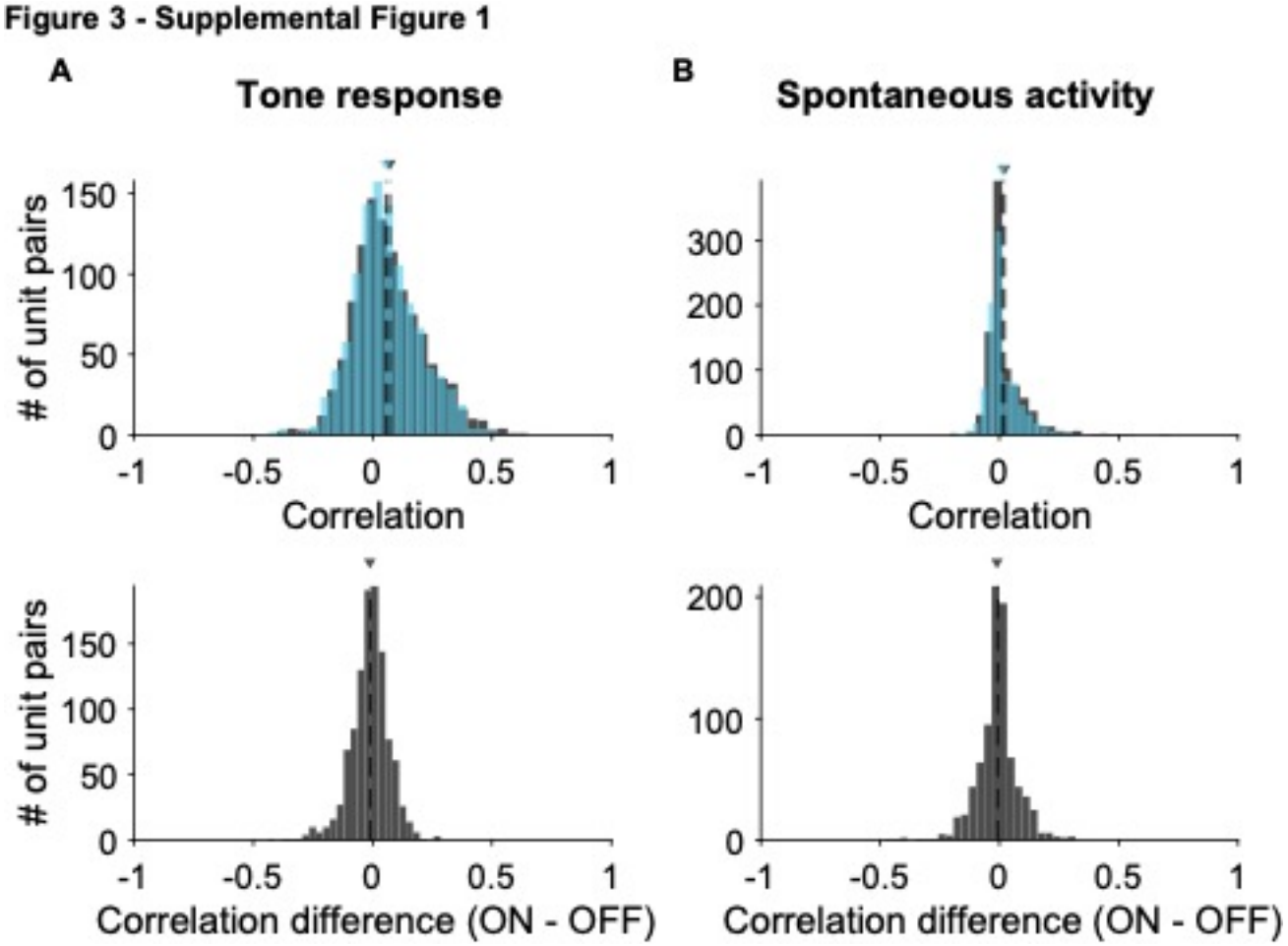

Figure 3 – Figure supplement 1. Effects of activating cortico-collicular feedback on noise correlations in IC. **A** TOP: Distribution of noise correlations of tone response for laser OFF (grey) condition (mean = 0.069) and laser ON (blue) condition (mean = 0.057) BOTTOM: Distribution of change in correlation between laser ON and laser OFF conditions (mean = -0.017). **B** TOP: Distribution of noise correlations of spontaneous activity for laser OFF (grey) condition (mean = 0.021) and laser ON (blue) condition (mean = 0.012) BOTTOM: Distribution of change in correlation between laser ON and laser OFF conditions (mean = -0.008).

Figure 3 - Supplemental Figure 2

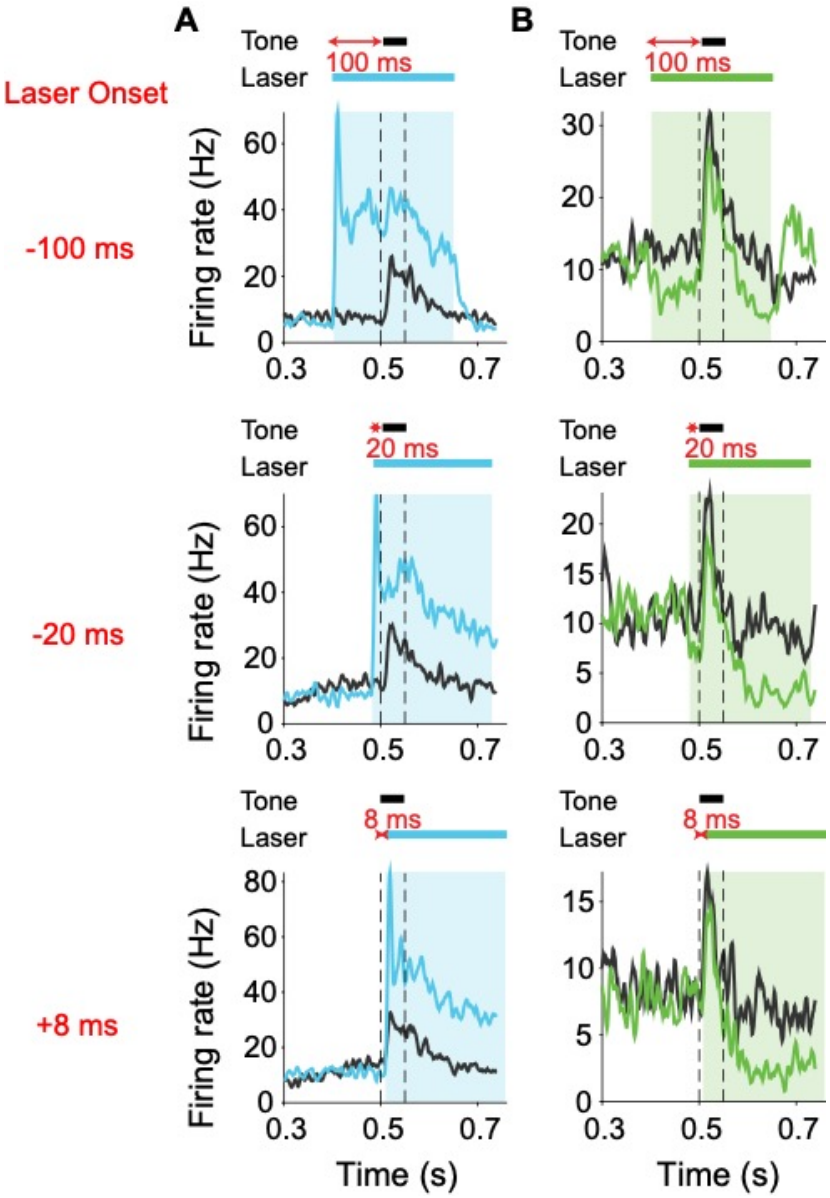

Figure 3 – figure supplement 2. Effects of modulating cortico-collicular feedback in AC on activity in AC in two example units. **A** Example unit with increased spontaneous and tone-evoked activity in AC with activation of cortico-collicular feedback in AC averaged across all frequencies. **B** Example unit with decreased spontaneous and tone-evoked activity in AC with suppression of cortico-collicular feedback in AC averaged across all frequencies.

Figure8 - Supplemental Figure 1

Inferior Colliculus

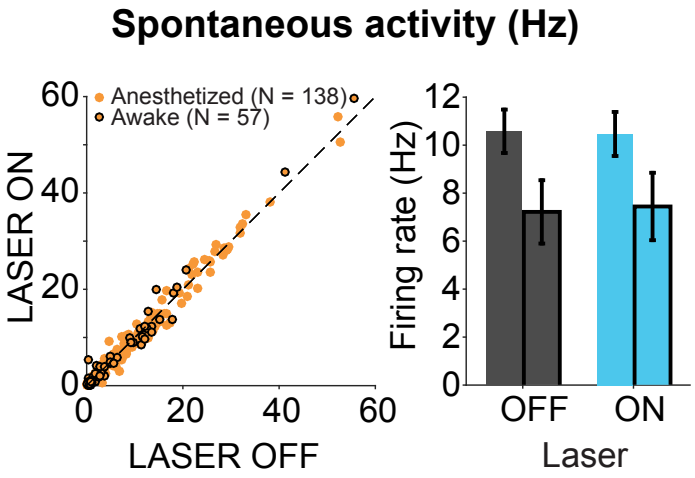

Auditory Cortex

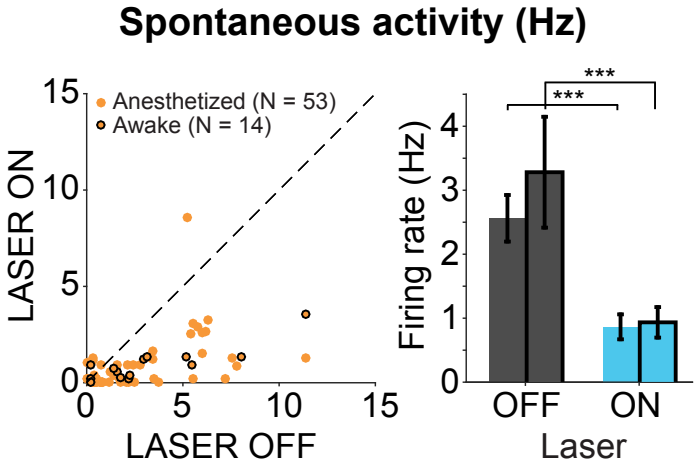

Figure 8 – figure supplement 1. Effects of activating PV interneurons in AC on spontaneous activity in IC (top) and AC (bottom) in both anesthetized and awake (black edges) preparations. TOP: Activation of PV interneurons in AC had no effect on spontaneous activity in IC for either awake (N = 57 units, ON = 7.4 ± 1.4 Hz, OFF = 7.2 ± 1.3 Hz) or anesthetized (N = 138, ON = 10.5 ± 0.92 Hz, OFF = 10.6 ± 0.9 Hz) recordings. BOTTOM: Activation of PV interneurons in AC decreased spontaneous activity in AC for both awake (N = 14, p = 8.5e-4, ON = 0.93 ± 0.24 Hz, OFF = 3.3 ± 0.87 Hz) and anesthetized (N = 53, p = 2.2e-7, ON = 0.87 ± 0.19, OFF = 2.6 ± 0.36) recordings.

.079

.080